Available online at www.sciencedirect.com

ScienceDirect

Geochimica et Cosmochimica Acta 225 (2018) 146–175

Geochimica et Cosmochimica Acta

www.elsevier.com/locate/gca

Chemical weathering outputs from the flood plain of the Ganga

Michael J. Bickle [a,*], Hazel J. Chapman [a], Edward Tipper [a], Albert Galy [b], Christina L. De La Rocha [c], Talat Ahmad [d]

[a] Department of Earth Sciences, University of Cambridge, Downing Street, Cambridge CB2 3EQ, United Kingdom
[b] CRPG – CNRS – Université de Lorraine, BP20, 54501 Vandœuvre-lès-Nancy Cedex, France
[c] Neu-Sophienhof 4B, 24256 Fargau-Pratjau, Germany
[d] Office of the Vice Chancellor, Jamia Millia Islamia, New Delhi 110025, India

Received 11 January 2017; accepted in revised form 4 January 2018; available online 12 January 2018

Abstract

Transport of sediment across riverine flood plains contributes a significant but poorly constrained fraction of the total chemical weathering fluxes from rapidly eroding mountain belts which has important implications for chemical fluxes to the oceans and the impact of orogens on long term climate. We report water and bedload chemical analyses from the Ganges flood-plain, a major transit reservoir of sediment from the Himalayan orogen. Our data comprise six major southern tributaries to the Ganga, 31 additional analyses of major rivers from the Himalayan front in Nepal, 79 samples of the Ganga collected close to the mouth below the Farakka barrage every two weeks over three years and 67 water and 8 bedload samples from tributaries confined to the Ganga flood plain. The flood plain tributaries are characterised by a shallow $\delta^{18}O$ - δD array, compared to the meteoric water line, with a low δD_{excess} from evaporative loss from the flood plain which is mirrored in the higher δD_{excess} of the mountain rivers in Nepal. The stable-isotope data confirms that the waters in the flood plain tributaries are dominantly derived from flood plain rainfall and not by redistribution of waters from the mountains. The flood plain tributaries are chemically distinct from the major Himalayan rivers. They can be divided into two groups. Tributaries from a small area around the Kosi river have $^{87}Sr/^{86}Sr$ ratios >0.75 and molar Na/Ca ratios as high as 6. Tributaries from the rest of the flood plain have $^{87}Sr/^{86}Sr$ ratios ≤0.74 and most have Na/Ca ratios <1. One sample of the Gomti river and seven small adjacent tributaries have elevated Na concentrations likely caused by dissolution of Na carbonate salts. The compositions of the carbonate and silicate components of the sediments were determined from sequential leaches of floodplain bedloads and these were used to partition the dissolved cation load between silicate and carbonate sources. The $^{87}Sr/^{86}Sr$ and Sr/Ca ratios of the carbonate inputs were derived from the acetic-acid leach compositions and silicate Na/Ca and $^{87}Sr/^{86}Sr$ ratios derived from silicate residues from leaching. Modelling based on the $^{87}Sr/^{86}Sr$ and Sr/Ca ratios of the carbonate inputs and $^{87}Sr/^{86}Sr$ ratios of the silicates indicates that the flood plain waters have lost up to 70% of their Ca (average ~ 50%) to precipitation of secondary calcite which is abundant as a diagenetic cement in the flood plain sediments. 31% of the Sr, 8% of the Ca and 45% of the Mg are calculated to be derived from silicate minerals. Because of significant evaporative loss of water across the flood plain, and in the absence of hydrological data for flood plain tributaries, chemical weathering fluxes from the flood plain are best calculated by mass balance of the Na, K, Ca, Mg, Sr, SO_4 and $^{87}Sr/^{86}Sr$ compositions of the inputs, comprising the flood plain tributaries, Himalayan rivers and southern rivers, with the chemical discharge in the Ganga at Farakka. The calculated fluxes from the flood plain for Na, K, Ca and Mg are within error of those estimated from changes in sediment chemistry across the flood plain (Lupker et al., 2012, Geochemica Cosmochimica Acta). Flood plain weathering supplies between 41

* Corresponding author.
E-mail address: mb72@esc.cam.ac.uk (M.J. Bickle).

https://doi.org/10.1016/j.gca.2018.01.003

and 63% of the major cation and Sr fluxes and 58% of the alkalinity flux carried by the Ganga at Farakka which compares with 24% supplied by Himalayan rivers and 18% by the southern tributaries.

Keywords: Ganga; Floodplain; Chemical weathering; Chemical discharge

1. INTRODUCTION

Chemical weathering on the continents supplies chemical fluxes to the oceans. Arguably the most important of these is the bicarbonate flux resulting from weathering of silicate minerals which results in the long-term removal of CO_2 from the oceans and atmosphere by precipitation of carbonate minerals in the oceans. This is thought to provide the temperature-sensitive feedback which has maintained equable surface temperatures over much of Earth-history although the relative importance of ocean floor carbonation, and organic carbon burial is a matter of debate (e.g. Chamberlin, 1899; Walker et al., 1981; Berner et al., 1983; François and Walker, 1992; Brady and Gíslason, 1997; Sleep and Zahnle, 2001; Galy et al., 2007; Coogan and Dosso, 2015). However it has proved difficult to determine the sensitivity of continental silicate chemical weathering to climatic (such as runoff and temperature) and other potential controls such as physical erosion and vegetation (e.g. White and Blum, 1995) and indeed, even to calculate the fraction of the total chemical weathering flux supplied by carbonic acid weathering of silicate minerals given the larger fraction derived from carbonates (e.g. Jacobson et al., 2002; Bickle et al., 2015). Carson and Kirby (1972) and Stallard and Edmond (1983) concluded that the crust could be subdivided into (1) 'transport-limited' weathering regimes in which exhumation and physical erosion were slow compared to chemical weathering rates such that chemical weathering rates were limited by the supply of material and (2) 'weathering-limited' regimes in which supply of material is fast such that material is incompletely weathered during transport through the river catchment. West et al. (2005) quantified this by parameterising silicate chemical weathering sensitivity to temperature, runoff and physical erosion rate and identified that rapidly eroding mountain belts dominated the 'weathering limited' regimes. The distinction is important because it is only in these that silicate chemical-weathering rates will respond to climatic forcing factors as in the 'transport-limited' regimes the eroded material is effectively completely weathered. It is for this reason that much attention is paid to the controls on silicate chemical weathering rates in rapidly eroding mountain belts. An important question which we address here is whether the continued weathering of the eroded Himalayan detritus in the flood plain of the Ganga is also 'weathering limited'.

It has been suggested that exhumation of the Himalayan-Tibetan orogen has been responsible, or partly responsible, for the marked cooling of climate over the Cenozoic. The increased physical erosion may have increased the 'weatherability' of the continental crust decreasing the global temperatures required to balance solid Earth CO_2 outgassing (Chamberlin, 1899; Raymo et al., 1988; Caldeira et al., 1993; Bickle, 1996). Alternatively solid-earth CO_2 outgassing from metamorphic decarbonation reactions in the orogen may have offset the cooling related to the increased 'weatherability' (e.g. Kerrick and Caldeira, 1993; Becker et al., 2008). A further impact of chemical weathering in the Himalayan-Tibetan orogen is on the seawater Sr-isotopic record in which the marked increase in seawater $^{87}Sr/^{86}Sr$ ratios since 40 Ma is ascribed to weathering of the unusually radiogenic Sr from the old Himalayan crust (Edmond, 1992; Galy et al., 1999; Jacobson and Blum, 2000) although there is little agreement as to the extent that this reflects increased silicate weathering, weathering of carbonates which have unusually high $^{87}Sr/^{86}Sr$ ratios in the Himalayas or is driven by oxidation of sulphides and sulphuric acid weathering (Raymo and Ruddiman, 1992; Richter et al., 1992; Caldeira et al., 1993; Bickle, 1996; Galy et al., 1999; Bickle et al., 2001; Jacobson et al., 2002; Quade et al., 2003; Huh, 2010; Turchyn et al., 2013; Torres et al., 2014).

Despite the significance of chemical weathering in the Himalayas, fundamental questions remain to be answered about the weathering processes. Perhaps the most important of these is where the weathering takes place. The 10^6 km^2 catchment of the Ganga extends from glaciated mountains to an intensively cultivated flood plain but it is uncertain how the chemical weathering fluxes are partitioned across these climatic and geomorphological zones (cf. Bouchez et al., 2012). Floodplains have been invoked as a fundamental control on chemical weathering outputs (Pogge von Strandmann and Henderson, 2015). Further, most chemical weathering, even in rapidly eroding mountain belts, probably takes place along a range of shallow to deeper groundwater flow paths (e.g. Tipper et al., 2006; Calmels et al., 2011; Andermann et al., 2012) and knowledge of the flow paths and their hydrology will be important for modelling the nature and rates of the chemical reactions and nature of isotopic fractionations imposed by the processes (e.g. Maher, 2011; Fontorbe et al., 2013; Li et al., 2014).

The Ganga is typical of many major rivers draining large orogens where the sediment load is primarily derived in the rapidly exhuming high mountains by glacial erosion and landslides and then transported through an extensive low-altitude flood plain where material may continue to be chemically weathered. Galy and France-Lanord (1999) and Rai et al. (2010) estimate that silicate chemical weathering fluxes from all the Himalayan-derived material in the flood plain are about 50% of those from the mountains (calculated as weight fraction of silicate derived CaO, MgO, Na_2O, K_2O and SiO_2). West et al. (2002) compared small catchment studies in the mountains with the Ganga chem-

ical discharge calculated by Galy and France-Lanord (1999). West et al. estimated that silicate weathering fluxes from sediment derived from the most rapidly eroding units in the Himalayas, the High Himalayan Crystalline Series, in the Ganga flood plain are about 6 times those from weathering of the High Himalayan Crystalline Series in situ in the high mountains. Lupker et al. (2012a) used the difference in composition of suspended loads in the rivers entering the flood plain and the load carried by the Ganga at Hardinge Bridge in Bangladesh to estimate the flood plain chemical weathering inputs. This resolved dominant inputs of silicate Na and K in the flood plain but could not resolve the relative inputs of silicate-derived Mg and Ca. The magnitude of chemical weathering in the flood plain raises a further important question which is whether weathering in floodplains is transport limited and thus does not act as a feedback to regulate climate. West et al. (2002) assumed the weathering in the plain was transport limited without offering any evidence. Lupker et al. (2012a) inferred that the 'lower erosion rates or longer residence times favour a supply-limited regime ..' but that 'such inferences should nevertheless be confirmed by dedicated mineralogical observations.' Here we will conclude that weathering in floodplain is 'weathering' limited.

To attempt to resolve the significance of weathering on the flood plain we present a three year time-series sample set collected every two weeks in the Ganga below the Farakka barrage, present and discuss the controls on the chemical and isotopic compositions of the flood plain rivers, and compile new and published analyses of the southern tributaries to the Ganga and of major rivers in Nepal. Calculation of flood plain weathering fluxes directly from the difference between the river chemical fluxes from the Himalayas and southern tributaries and the output at Farakka is inaccurate because the runoff from the flood plain (rainfall less evapo-transpiration) is poorly defined and the difference between the inputs from the Himalayas and southern rivers and discharge at Farakka is too uncertain. It is concluded that the best estimates of the chemical and water inputs are based on mass balance calculations using the mean solute chemistry and Sr-isotopic compositions of the three input sources (1) Himalayan mountain rivers, (2) the southern tributaries and (3) the flood plain. All these are compared to the solute compositions of the Ganga at Farakka. An attempt is made to partition the chemical fluxes into those from carbonate minerals, silicate minerals and saline sources. The estimates of these flood plain chemical weathering fluxes are compared with those from the Himalayan mountains and the southern tributaries.

2. GEOLOGICAL SETTING AND PREVIOUS WORK

The Ganga flood plain above the Farakka sample site has an area of $\sim 4.1 \times 10^5$ km^2 with a further 0.9×10^5 km^2 downstream (Fekete et al., 2000; Fig. 1) and has a maximum elevation of ~300 m. The rest of the catchment is in the Himalayan mountains ($\sim 1.76 \times 10^5$ km^2) and on the Indian shield to the south ($\sim 3.5 \times 10^5 \times$ km^2) (Singh et al., 2008). The flood plain is densely populated with ~500 million people, intensively cultivated with numerous irrigation channels and contains major conurbations.

The chemistry of rivers and sediments in the flood plain and their impact on the chemical fluxes carried by the Ganga have been subject to a number of studies including Sarin et al. (1989), Palmer and Edmond (1992), Gupta and Subramanian (1994), Galy and France-Lanord (1999), Galy et al. (1999), Singh et al. (2004, 2005b, 2009), Rai et al. (2010), Garzanti et al. (2010, 2011) and Lupker et al. (2012a).

The flood plain is bounded to the north by the Himalayan mountain chain. This rises abruptly above the active main frontal thrust to elevations of 2–3 km over thrust complexes of the syn-orogenic Siwalik sediments and low-grade continental sediments of the mainly Proterozoic Lesser Himalayan Series. Further north the topography steepens across the inactive south-verging Main Central Thrust which has emplaced the amphibolite-facies kyanite to sillimanite and migmatitic metasediments and gneisses of the Late-Proterozoic and Early Palaeozoic High Himalayan Crystalline Series. The upper reaches of the major rivers draining the Himalayas cut through the highest mountains comprising High Himalayan Crystalline Series and extend onto the Tibetan Plateau where their catchments are underlain by the mainly low grade Phanerozoic continental margin sequence of clastic and carbonate rocks known as the Tibetan Sedimentary Series. The Deccan plateau to the south of the Ganga flood plain comprises Proterozoic orogenic belts overlain by Deccan plateau basalts. The Ganga is fed by seven major rivers which penetrate the Himalayas to the north and by six major rivers which rise on the Deccan plateau to the south (Fig. 1).

3. SAMPLE COLLECTION AND ANALYTICAL METHODS

Analyses of water samples are listed in Electronic annex Table E1. Water samples from rivers rising on the Ganga flood plain as well as the some of major rivers rising in the Himalayas and the southern tributaries (Chambal, Kunwari, Betwa, Tons and Son) to the Ganga were collected from bridges, boats or river banks in August 2003 and August 2005, filtered through 0.2 μm nylon filters with one aliquot acidified with ultrapure HNO_3 and one aliquot kept unacidified for analysis of anions. pH and water temperature were measured at the sample site. Alkalinity was measured on a subset of the 2005 samples by Gran titration on the day of collection. The silicon concentrations and silicon isotopic compositions of a subset of the Ganga flood plain samples collected in 2003 were discussed by Fontorbe et al. (2013). Samples from the Ganga mainstem Farakka site were collected 1 km downstream of the barrage (87.93065° E, 24.76072° N) approximately twice a month between December 2005 and February 2009, filtered on site with one 60 ml sample acidified with ultrapure HCl and one 60 ml sample unacidified. Water samples in Nepal were collected from the Kosi at Chatra, the Karnali at Chisapani, the Rapti at Bhaluwang and the Narayani above Naryangadh in Nepal in July 2015, the Narayani in

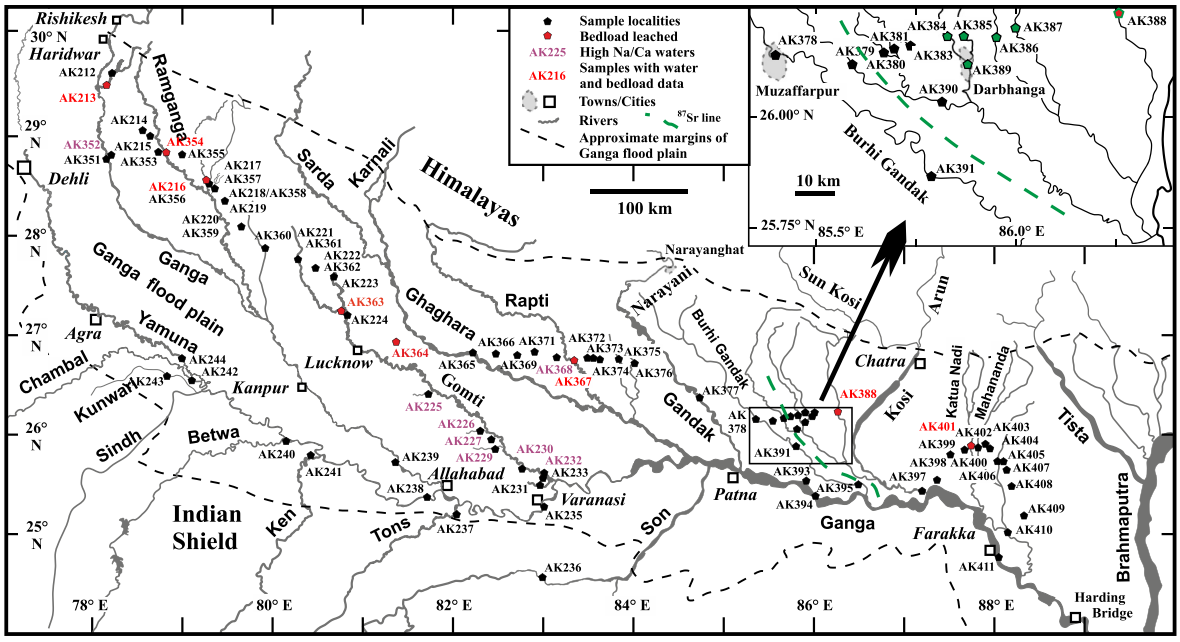

Fig. 1. Map showing major rivers and sample localities in the Ganges flood plain. Based on US Army Map Service (GDVLB) (1955) 1:250,000 sheets. Sample sites with bedload leaches and residues analysed shown with red symbols. High Na/Ca water samples in magenta. Green dashed line denotes western boundary of high-$^{87}Sr/^{86}Sr$ tributaries on flood plain (division between West and East Kosi samples- see text).

September 2015 and the Narayani and Kosi in June and August 2016. These samples were filtered through 0.2 μm polyethersulfone filters, one 250 ml sample acidified with ultrapure HNO_3 and a 60 ml sample kept unacidified for analysis of anions. pH and water temperature were measured at the sample site and an aliquot titrated for carbonate alkalinity (Gran titration) within 12 h of collection.

The acidified filtered water samples were analysed for the elements Na, K, Ca, Mg, Si, S, Sr, by inductively coupled plasma-atomic emission spectroscopy at Cambridge, the Ganga flood plain samples on a Varian Vista ICP-OES and the 2015 and 2016 Nepal samples on an Agilent 5100 ICP-OES. Calibration was against mixed standards made up from ICP-MS standards with cation proportions specifically designed to match the waters to minimise matrix effects. The analyses are given in Electronic annex: Table E1 which includes analyses of international water standards run at the same time as the samples. All samples were analysed in two separate runs with reproducibility within 2%.

Anions (Cl, SO_4, NO_3, F) were analysed either on a Dionex ion chromatograph at the Open University (2003 Ganges flood plain samples) where repeat measurements indicate precisions of better than 10% on Cl, N and S and 30% on F, or a Dionex ICS-3000 ion chromatograph at Cambridge where repeat measurements of USGS natural river water standard T-143 gave reproducibility better than 4% (2SD, n = 97) (2005 Ganga flood plain samples and the Farakka samples). S measured by emission spectroscopy and ion chromatography reproduced with a mean standard deviation of ~4%. Anions in the 2015 and 2016 Nepal samples were analysed on a Dionex ICS-5000+ system in Cambridge using a high capacity hydroxide-selective column (IonPac AS18) with a KOH eluent at a flow rate of 1 ml/min with a precision calculated from replicates of ~2%. $\delta^{18}O$ and δD were analysed on the unacidified samples at Cambridge in December 2015 by cavity ring down spectroscopy using a L1102-*I* Picarro water isotope analyser and A0211 high-precision vaporizer at the Godwin Laboratory for Palaeoclimate Research at the University of Cambridge using protocols described by Hodell et al. (2012). Internal standards were calibrated against V-SMOW, GISP, and SLAP and results are reported in parts per thousand (‰) relative to V-SMOW. The reproducibility of the method was 0.07 ‰ for $\delta^{18}O$ and 0.55 ‰ (1σ) for δD, estimated by repeated analysis (n = 48) of an internal standard run together with the samples. The older samples had been stored in a cold room (5 °C) for up to twelve years with a variable headspace. Samples reanalysed for cation and anion concentrations after several years storage exhibit undetectable changes in concentration and 5% evaporation would cause negligible isotopic fractionations of $\delta^{18}O$ and δD.

Strontium was separated using Dowex 50Wx8 cation exchange resin with 200–400 mesh particle size in clean lab conditions and $^{87}Sr/^{86}Sr$ ratios were measured on a VG Sector 54 solid source mass-spectrometer using a triple-collector dynamic algorithm, normalised to $^{88}Sr/^{86}Sr$ 0.1194 with an exponential fractionation correction (cf. Bickle et al., 2003, 2005). The 402 analyses of NBS 987 during the 12 year period over which the 2003, 2005, Farakka Barrage, bedload and Nepalese samples were analysed gave a mean value of 0.710262 ± 9 (1σ). 13 analyses of NBS987 made in 2016 during the analyses of the Nepal samples gave a mean of 0.710271 ± 7 (1σ). Sr blanks for analyses of

waters and bedloads were <700 pg except for acetic acid leaching which had a blank up to 1.4 ng but all these were negligible given the mass of Sr separated.

Bedloads were sampled as recently deposited sand-sized material exposed on sand banks or river banks. Analyses of leaches and residues of bedload (Electronic annex material: Table E2) followed Bickle et al. (2015, Table 1) with samples initially washed in water to remove loosely held cations, then leached in cold 10% acetic acid which dissolves most of the calcite and a significant fraction of dolomite, then leached in cold 1 M HCl to remove remaining carbonate. The silicate residue is rinsed and dissolved in pressure vessels in 3 stages with 48% HF + $HN0_3$, 6 M HNO_3 and finally 6 M HCl. The acids used are quartz distilled except Romil-UpA™ HF. The solutions were analysed for major and trace cations by ICP-OES using concentration-matched standards and for $^{87}Sr/^{86}Sr$ ratios with the same method as for the water samples. Several of the bedload samples (AK213, AK216, AK354, AK363, AK401) contained negligible Ca and presumably negligible calcite and the leach contains significant silicate-derived cations.

Concentrations of major ions in waters are quoted as μmoles/L except for Sr which is quoted as nmoles/L. Element ratios in waters are quoted as molar ratios except for Sr/Ca which is quoted as mmol/mol (1000Sr/Ca). In discussions of weathering processes of the flood plain tributaries below, the compositions have been corrected for chemical inputs by rain and saline sources. The corrections follow standard methods (e.g. Galy and France-Lanord, 1999; Gaillardet et al., 1999; Bickle et al., 2005; Chapman et al., 2015). Rain inputs are based on the average rain water composition in the Ganga flood plain compiled by Galy and France-Lanord (1999), and for Sr and $^{87}Sr/^{86}Sr$ ratios the average Bangladesh rain in Galy et al. (1999). The concentrations of these solutes were all multiplied by two to account for evapo-transpiration (Krishnamurthy and Bhattacharya, 1991, see below). The Cl remaining after the correction for rain inputs was assumed to be derived from an evaporite-like source with the Na/Cl, K/Cl, Ca/Cl, Mg/Cl, Si/Cl, Sr/Cl ratios of Himalayan hot springs compiled by Bickle et al. (2005). The correction has been applied to the mean flood plain water composition (Table 1) and the individual tributaries. The important correction is to Na concentrations where ~30% on average is estimated to be derived from rain and saline sources compared to 22% for Ca, 12% for Mg and 10% for Sr. Corrected $^{87}Sr/^{86}Sr$ ratios are reduced by an average of 0.001 for the West Kosi samples and 0.009 for the much higher $^{87}Sr/^{86}Sr$ ratio East Kosi samples.

4. GANGA CHEMICAL FLUXES: FARAKKA TIME SERIES SAMPLING

The analyses of water samples collected approximately twice a month for three years at Farakka on the Ganga were averaged by month (Figs. 2 and 3). Concentrations of the cations Na, Ca, Mg and Sr exhibit systematic variations with a decrease in concentration during the monsoon to between 26% (Na) to 56% (Ca) of the dry season values (Fig. 2A). This compares to the 20-fold increase in discharge during the monsoon. K and Si exhibit more complex variations (Fig. 2B). The average monthly discharge of the Ganga at Farakka has been estimated from monthly discharge data measured between 1949 and 1972 (Hossain et al., 1987). The concentrations of most of the elements exhibit characteristic hysteresis with concentrations rapidly diluted during the first part of the discharge, increasing between March and June but then stabilising during July and August. During the waning discharge between August and November the concentrations are substantially higher than during the first part of the cycle (Fig. 3). This differs from the chemostatic behaviour observed in some rivers (Maher, 2011). K and Si exhibit rather different patterns from the other cations with K exhibiting a non-linear correlation directly with discharge and Si an irregular but rapid drop in concentration prior to the Monsoon (June), values rise with increasing discharge to July, remain approximately constant during the rest of the Monsoon (August to October) and rise with falling discharge during the latter part of the year.

The hysteresis implies the changes in concentration are not simply due to dilution during the monsoon (Fig. 4). The marked drop in Na/Ca, Mg/Ca and Sr/Ca from May to July at the start of the monsoon is consistent with an increase in the fraction of cations derived from carbonate weathering observed in Himalayan catchments during the monsoon (Tipper et al., 2006). In contrast to this Si/Ca increases prior to the Monsoon although this increase starts earlier (March) and is less marked. K/Ca rises from March to May. $^{87}Sr/^{86}Sr$ increases from April to July, drops in August and then increases to October. It is probable that the changes in chemistry represent both changes in the relative inputs from the Himalaya, the southern tributaries and flood plain weathering combined with seasonal changes in weathering processes.

The contrasting compositions of the Ganga and its major tributaries are illustrated in Fig. 5 which shows compositions of the major flood plain rivers sampled in August 2003 or 2005 against distance downstream from Rishikesh. The Yamuna with a discharge ~50% higher than the Ganga above Allahabad dominates Sr and $^{87}Sr/^{86}Sr$ ratios.

The discharge-weighted mean composition of the Ganga at Farakka was calculated from the mean monthly chemistries weighted by the mean monthly discharges (data between 1949 and 1972) at Harding Bridge (Hossain et al., 1987) (Table 1).

The uncertainties in the composition of the Ganga are calculated by a Monte Carlo routine (detailed in Electronic annex: Calculation of chemical fluxes, see also Chapman et al., 2015) in which the 1σ uncertainty on the relative monthly discharges is taken as 25%, the average variability of monthly discharges of the time series data of Hossain et al. (1987). The uncertainties on the element concentrations are taken as the standard errors on the monthly means.

5. GANGES FLOOD PLAIN TRIBUTARY CHEMISTRIES

The objective of sampling flood plain rivers was to sample waters whose compositions reflected the weathering

Table 1
Discharge-weighted mean composition of Ganga at Farakka and floodplain rivers.

Sample	Na	1se	K	1se	Ca	1se	Mg	1se	Si	1se	Cl	1se	SO_4	1se	NO_3	1se	F	1se	Sr	1se	$^{87}Sr/^{86}Sr$	1se (ppm)
	μmol/L																		nmol/L			
Ganga at Farakka	364.0	11.5	83.3	0.8	726.4	9.8	293.2	5.7	148.9	4.8	126.5	5.6	117.7	2.6	36.5	3.8	9.9	0.2	1136.5	27.5	0.72662	0.00040
Flood Plain West Kosi[a]	542.5	51.4	101.6	16.2	777.5	44.7	384.0	40.7	189.5	10.7	114.4	13.0	94.1	13.7	22.1	5.9	12.5	0.7	1211.9	80.0	0.73000	0.00087
Flood Plain East Kosi[a]	206.7	18.1	53.8	5.7	284.7	50.0	127.3	20.4	128.8	13.7	67.5	5.8	28.5	5.2	3.8	1.5	10.2	0.4	320.5	35.6	0.75293	0.00112
Flood Plain average[b]	521.5	48.2	98.6	15.2	746.7	42.0	368.0	38.2	185.7	10.1	111.5	12.2	90.0	12.8	21.0	5.5	12.3	0.7	1156.2	75.0	0.73040	0.00086

[a] West Kosi and East Kosi regions (see Fig. 1).
[b] Averaged proportional to floodplain areas with West Kosi area being 0.9375 of total floodplain to Farakka barrage.

processes on the flood plain. However the hydrology of the flood plain may mix waters from the Himalayan mountains with flood plain waters. The extensive network of irrigation channels across the Ganges flood plain supplied from reservoirs in the Himalayas or from the major Himalayan rivers is likely to enhance such mixing. During the monsoon the major Himalayan rivers flood extensive areas (widespread flooding was observed around the lower reaches of the Kosi during the 2005 sample collection). Flood plain rivers and mountain rivers are distinct in $\delta^{18}O$ and δD (Section 5.1) suggesting any mixing is limited. We discuss regional variations in flood plain river chemistries, the extent of precipitation of secondary carbonates in the flood plain and the quantification of the chemical inputs from rain, saline, anthropogenic sources and weathering of carbonate and silicate minerals.

5.1. Oxygen and hydrogen isotope compositions of mountain and flood plain waters

Small flood plain tributaries, the major rivers from Nepal and precipitation in the Gangetic plain define distinct correlations (Fig. 6). The Nepal data includes both that from the present study in addition to published analyses of major Nepalese rivers (Gajurel et al., 2006). The flood plain rivers include those sampled in 2003 and 2005 as well as three samples of the Gomti in the flood plain from Gajurel et al. (2006). The δD_{excess} (calculated as $\delta D_{excess} = \delta D - 8^{*}\delta^{18}O$, Dansgard, 1964) of the flood plain rivers $= 5.5 \pm 0.6‰$ ($n = 74$), precipitation $= 8.8 \pm 1.0‰$ ($n = 71$) and the Nepalese rivers $= 12.3 \pm 0.8‰$ ($n = 47$) (2x standard error). The slope of the δD correlation with $\delta^{18}O$ of 8.03 ± 0.36 (2 x standard error) for the precipitation is typical for the meteoric water line (MWL) (Craig, 1961).

The difference between the flood plain rivers with low δD_{excess} and the major Nepalese rivers with high δD_{excess} is consistent with evaporative increases in δD and $\delta^{18}O$ of the flood plain waters with corresponding decreases in δD and $\delta^{18}O$ of the vapour which then precipitates in the mountains. The rotation of the correlations for both the flood plain rivers and the major Nepalese rivers to lower slopes than the MWL is a consequence of this, as evaporation at humidities of ~80% characteristic of the flood plain (e.g. Kumar et al., 2010) fractionates vapour and residual water along slopes of ~5 (Craig and Gordon, 1965). Krishnamurthy and Bhattacharya (1991) used the gradient in $\delta^{18}O$ of precipitation across the Ganga flood plain (sampled as groundwaters) to estimate that ~30% of the vapour flux entering the Ganga flood plain at Kolkata is lost by precipitation as it passes across the flood plain but that ~40% of the precipitation which falls is re-evaporated. If the re-evaporation is directly from the ground this would fractionate δD and $\delta^{18}O$, but if the evaporation is through vegetation (transpiration) this would not cause fractionation (e.g. Dawson et al., 2002) and thus the isotopic shift may not reflect the total re-evaporation flux.

The difference in δD_{excess} between the flood plain waters and the mountain rivers compared to the local meteoric water line confirms that the water in small flood plain rivers

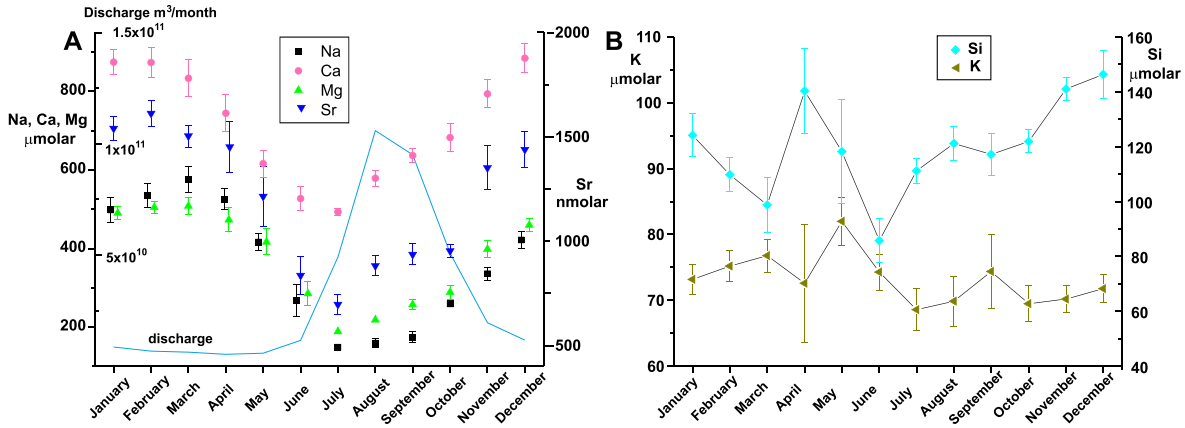

Fig. 2. (A) Variations in average monthly rain- and salt-corrected Na, Ca, Mg, and Sr and, (B) K and Si, in the Ganga below Farakka. Error bars are 1 standard error about mean. Blue line shows mean monthly discharge of the Ganga at Harding Bridge, Bangladesh, between 1949 and 1972 after Hossain et al. (1987).

is predominantly derived from precipitation in the flood plain and not redistributed from the major mountain rivers via ground water or irrigation systems.

5.2. Spatial trends in flood plain waters based on Na/Ca and $^{87}Sr/^{86}Sr$ ratios and bedload chemistries

Most of the flood plain tributaries have rain- and evaporite-corrected Na/Ca molar ratios between ~0.2 and 1.0, with the average of flood plain waters with Na/Ca < 1.0 being 0.41 ± 0.21 (1σ) (Fig. 7, Table 1). A limited number of samples exhibit higher Na/Ca ratios. The flood plain tributaries may be divided into two sets on the basis of their $^{87}Sr/^{86}Sr$ ratios with samples from a limited area around the Kosi river having $^{87}Sr/^{86}Sr$ ratios and most Na/Ca ratios significantly higher than those to the west (Figs. 1 and 7C, D, Table 1). The discussion of the flood plain river chemistry is divided into two areas, (1) the majority of the floodplain to the west of a line shown on Fig. 1 which runs just to the west of the Kosi termed the 'West Kosi' samples and (2) the remaining rivers termed the 'East Kosi' samples. The high $^{87}Sr/^{86}Sr$ ratios of ~0.77 from the acetic acid leaches of East Kosi bedload samples AK388 and AK401 are consistent with Sr in these bedload samples, and the river waters, being derived predominantly from the Lesser Himalayan units. These contain silicate minerals and dolomitic calc-silicates with very elevated carbonate $^{87}Sr/^{86}Sr$ ratios (e.g. Singh et al., 1998; Galy et al., 1999; English et al., 2000; Bickle et al., 2001; Quade et al., 2003). The Mg/Ca molar ratios of the acetic acid leaches of AK388 and AK401 of ~0.5 (Electronic annex Table E2) are consistent with dolomite comprising two-thirds of the carbonate leached from these bedload samples. Note that the HCl leaches only removed ~15% of the total (acetic and HCl) acid-leached Ca and the acetic acid leaches therefore represent the majority of the sample carbonate. Lupker et al. (2012a) report that the major Himalayan and flood plain rivers have dolomite fractions of the total carbonate in the bedload between 23 and 82% with the samples taken from the Kosi containing highest fraction of dolomite. The two West Kosi water samples with high $^{87}Sr/^{86}Sr$ ratios (AK217 and AK357) were collected in the northern part of the flood plain and likely reflect similar local dominance of Lesser Himalayan sediment inputs.

The East Kosi water samples exhibit a coherent trend in Sr/Ca versus Na/Ca which approximates the compositions of mixtures of the carbonate and silicate fractions of the bedload. The three highest Sr/Ca and Na/Ca samples, which lie above the bedload trend, may have had their Sr/Ca ratios elevated by precipitation of secondary calcite (see discussion in Bickle et al., 2015 and in Section 5.4.4 below). The East Kosi samples also exhibit a positive correlation between $^{87}Sr/^{86}Sr$ and Na/Ca ratios where the samples with elevated Na/Ca have $^{87}Sr/^{86}Sr$ ratios within the range of the silicate residue compositions.

5.3. Na-rich tributaries to the Gomti and Na-salts

Eight out of the forty-eight West Kosi samples have rain and salt-corrected Na/Ca > 1.1 and lie on a trend of increasing Sr/Ca with increasing Na/Ca but with a lower slope than the array of silicate residues (Fig. 7A, see also Electronic Annex, Fig. E2). The $^{87}Sr/^{86}Sr$ ratios of these samples decrease with increasing Na/Ca (Fig. 7C). Most of these samples are from small tributaries on the flood plain south of the Gomti and one downstream sample of the Gomti (Fig. 1). The samples collected in August from the upstream Gomti have rain and Na-salt corrected Na/Ca ratios just less than 1. Previous sampling of the Gomti during the dry seasons has yielded high Na/Ca ratios between 1.1 and 3.7 (Gupta and Subramanian, 1994; Singh et al., 2005a, 2009). However Na/Ca ratios in the Gomti during the monsoon are lower with Subramanian et al. (1987) reporting a Na/Ca ratio of 0.71 and the Gomti samples in this study ranging from Na/Ca = 0.40 upstream to 1.52 downstream. The Gomti tributaries sampled by this study during the monsoon have rain and salt-corrected Na/Ca ratios between 0.44 and 4.15 with the set of tributaries on the west bank downstream of Lucknow (AK225 to 230) exhibiting uniformly high values of 2.4 to 4.1. The very high Na/Ca ratios are associated with low Sr/Ca, Mg/Ca and K/Ca ratios (Electronic annex Fig. E2). It is likely that

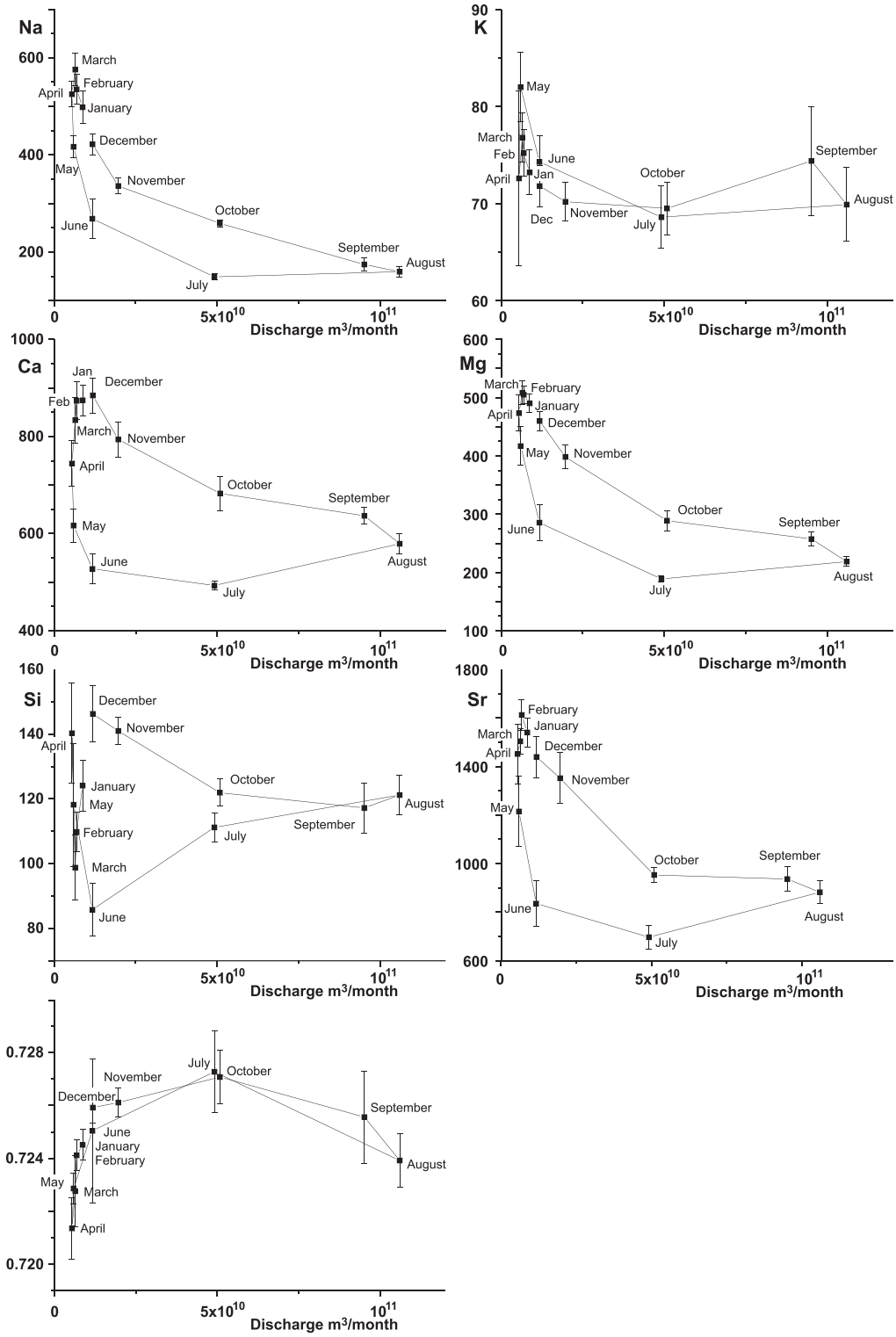

Fig. 3. Average monthly concentration versus average monthly discharge for rain- and salt-corrected cations, Si and $^{87}Sr/^{86}Sr$ in the Ganga at Farakka.

these waters are enriched in Na by leaching Na-bicarbonate or carbonate salts precipitated in the drier, western region of the flood plain during the dry season as reported for example by Pal et al. (2003) and reviewed by Rai et al. (2010).

The West Kosi flood plain tributaries with Na/Ca < 1.1 exhibit a scatter of compositions with a mean Na/Ca ratio of 0.43 ± 0.05 (1 x standard error). This ratio is significantly higher than the mean of the Himalayan derived rivers entering the flood plain of 0.18 ± 0.06 (1se) discussed

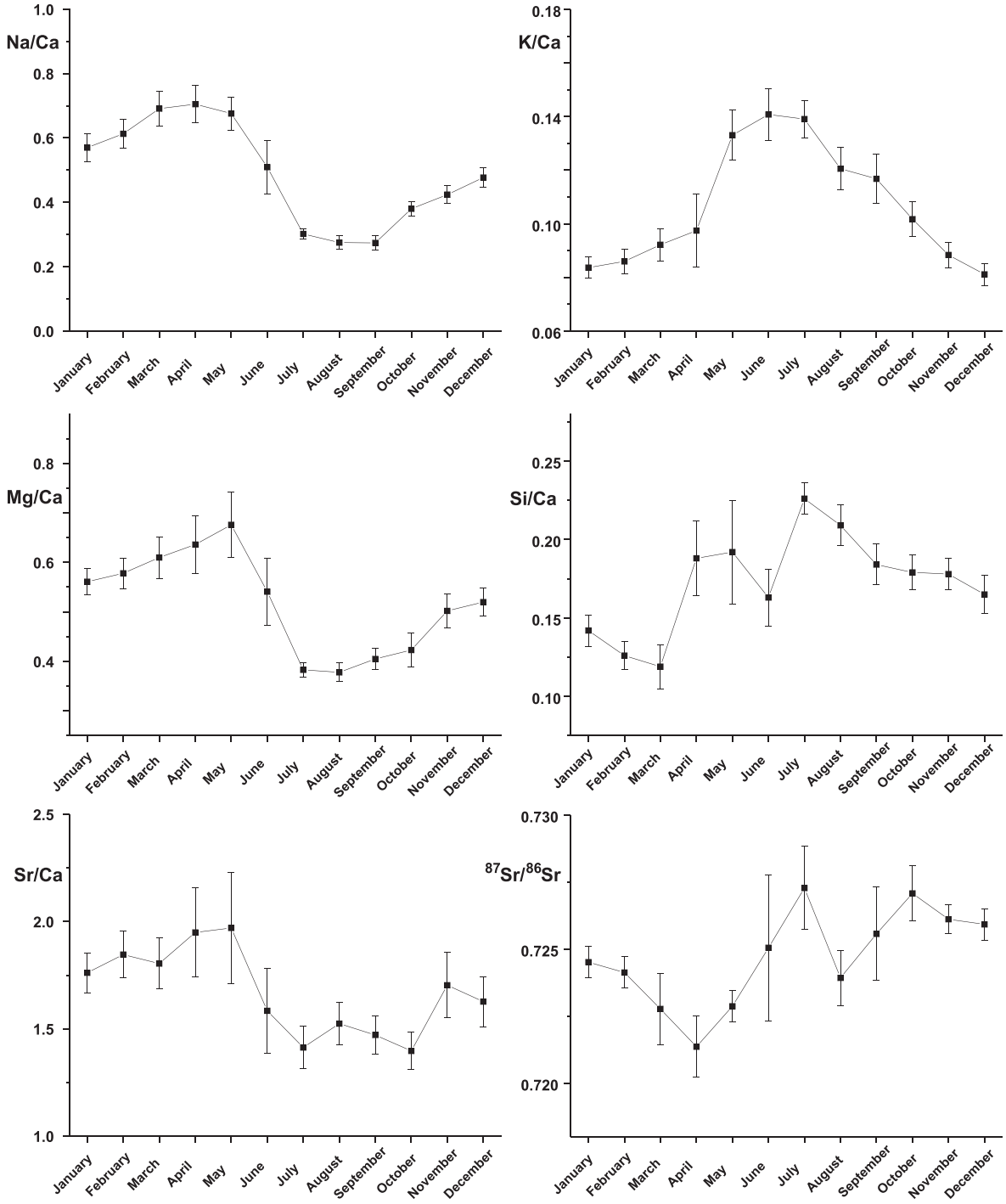

Fig. 4. Rain- and salt-corrected cation and Si ratios to Ca in the Ganga at Farakka. Mean monthly ratios with 1 x standard error about means.

below. Rai et al. (2010) argue that the elevation in Na primarily reflects addition of Na salts rather than increased silicate weathering on the basis of the low Si/Na ratios of the Gomti waters. However Si-isotopic ratios in the flood plain exhibit increases in δ^{26}Si values which Fontorbe et al. (2013) could only model with net loss of up to 50% of Si from the waters, implying further weathering of higher Al/Si silicate minerals with corresponding loss of Si to clay minerals, or by biological uptake. The low Si/Na ratios likely reflect loss of Si.

The high Na/Ca waters from the East Kosi exhibit trends which parallel the silicate residues from leaching

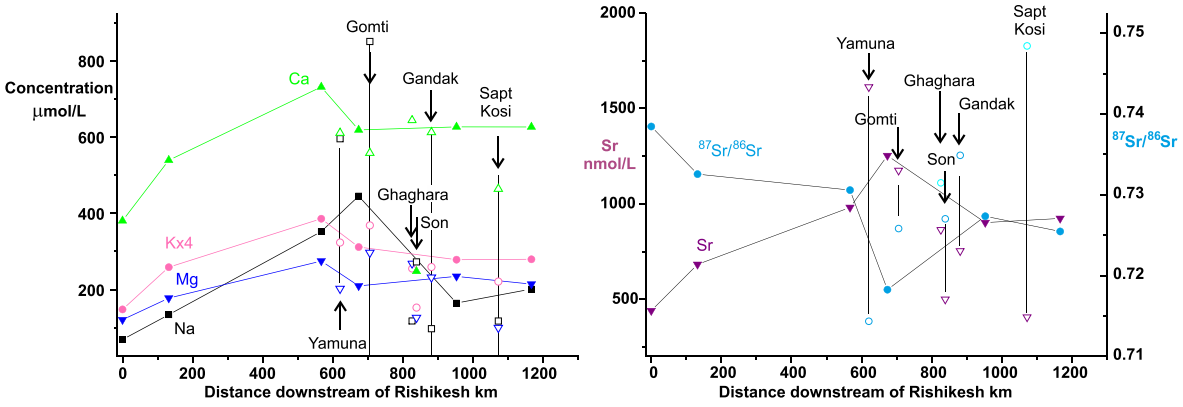

Fig. 5. Evolution of element and Sr-isotopic compositions of the Ganga downstream of Rishikesh for samples collected in August 2003 and 2005 (solid symbols). Major tributaries are shown with open symbols.

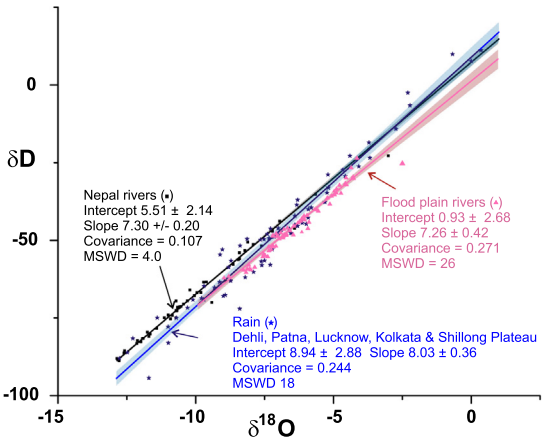

Fig. 6. δD-δ^{18}O compositions of flood plain rivers and major rivers from Nepal (Electronic annex Table E1) with additional data from 3 samples of the Gomti in the flood plain and major rivers from Nepal from Gajurel et al. (2006). Analyses of rain collected in Dehli, Patna, Kolkata and the Shillong Plateau from Battacharya et al. (1985) and Kumar et al. (2010). Linear regressions calculated using program of York (1969) using quoted analytical errors in δD and δ^{18}O. Error estimates on intercepts and slopes quoted at 2σ (also shown as coloured envelopes) are calculated with error estimates on δD and δ^{18}O increased to give expected Mean Squared Weighted Deviate (MSWD) = 1.

bedload implying the increase here in Na is primarily due to weathering of silicate minerals (Fig. 7A and C). The scatter in the West Kosi river waters with Na/Ca < 1.1 makes it difficult to distinguish inputs from silicate weathering from additions of Na salts but most of these samples lie above the trend of the Na/Ca > 1.1 West Kosi samples or predicted for the addition of Na salts which have very high Na/Ca, Na/Mg and Na/K ratios (e.g. Bhargava et al., 1981; Pal et al., 2003). A question which then arises is the extent to which the weathering yields from the flood plain are out of long-term equilibrium. Because the Na-enriched salts concentrated on the flood plain are primarily derived from silicate weathering (Pal et al., 2003) their return to the river waters completes the weathering cycle but their precipitation and subsequent dissolution may be climate and thus time dependent.

5.4. Calculation of relative weathering fluxes derived from carbonate and silicate minerals

Deconvolution of the chemical weathering flux into atmospheric, saline (evaporite or hot spring), carbonate and silicate mineral sources is important when determining the silicate chemical weathering flux which impacts CO_2 removal from the atmosphere and thus long-term climate. In addition there is considerable interest in the extent to which the high $^{87}Sr/^{86}Sr$ ratios of Himalayan river waters are derived from carbonate or silicate sources. However there is no accepted method for apportioning the major cations, Ca and Mg, between carbonate and silicate sources given the probable incongruent dissolution of the solid components. The calculations are complicated by the precipitation of secondary calcite (e.g. Jacobson et al., 2002; Bickle et al., 2015) which we discuss first. This section briefly reviews possible approaches and suggests calculations based on Sr/Ca ratios and $^{87}Sr/^{86}Sr$ ratios of the carbonate input allow estimates of the magnitude of precipitation of secondary calcite.

The flood plain tributaries scatter in a plot of Sr/Ca versus Na/Ca (Fig. 7B). Most lie above the correlation defined by acetic acid leaches, bulk sample and silicate residues from leaching, as is common in waters from the Himalayas (Galy et al., 1999; Jacobson et al., 2002; Bickle et al., 2005, 2015). The increase in Sr/Ca ratios above those of the source minerals is attributed to precipitation of secondary calcite. However the scatter of the flood plain waters precludes calculation of the loss of Ca, Sr and Mg to secondary calcite and partitioning cations between silicate and carbonate sources using the difference between correlations of water and bedload in Sr, Ca, Na, Mg and $^{87}Sr/^{86}Sr$ space as done by Bickle et al. (2015). Below we conclude that the scatter results both from variations in the amount of secondary calcite precipitation and from the heterogeneity in the silicate fractions of the bedload samples.

Calculation of the relative fractions of the cations derived from silicate and carbonate minerals depends on

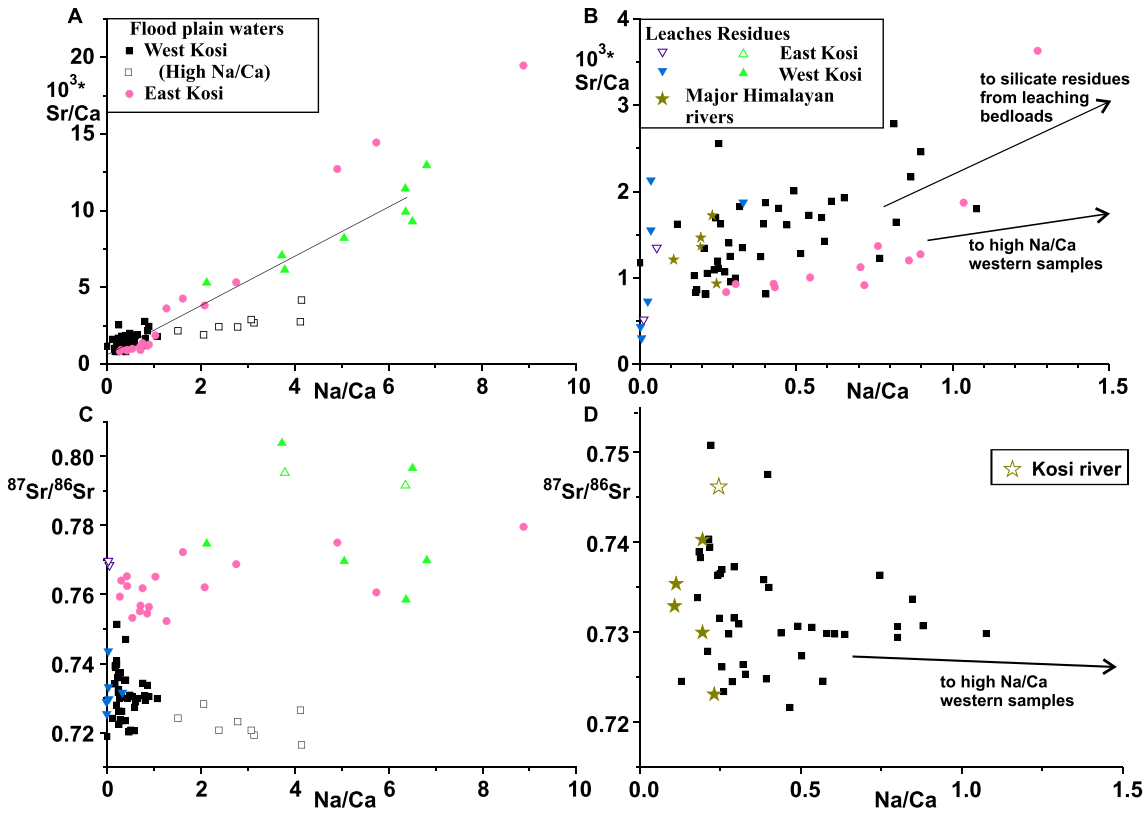

Fig. 7. Sr/Ca (mmol/mol) and $^{87}Sr/^{86}Sr$ versus Na/Ca rain- and evaporite-corrected molar ratios for tributaries which rise on the flood plain subdivided into those collected in the West Kosi region and in the East Kosi region (Fig. 1). (A and C) shows the compositions of the flood plain rivers and the composition of the silicate residues from leaching of the bedload samples. Least-squares best fit to East Kosi samples shown on (A). (B and D) shows a detail of the lower Na/Ca samples as well as the compositions of the acetic acid leaches of the flood plain bedload samples. Inverted blue triangles show acetic acid leach compositions and green triangles silicate residue from leaching subdivided into samples from West and East Kosi regions.

their end-member compositions but is complicated by the incongruent dissolution of both the silicate and carbonate mineral fractions. The significant silicate minerals in the suspended load of the mainstem Ganga, as sampled at the downstream Hardinge Bridge site, include plagioclase, K-feldspar, biotite, muscovite, chlorite and clay minerals (Garzanti et al., 2010, 2011; Garçon et al., 2014) of which plagioclase and biotite are likely to weather fastest. Garçon et al. (2014) indicate that the carbonate fraction from the downstream Ganga mainstem contains about equal weight fractions of calcite and dolomite (dolomite 35% mole fraction) which is consistent with dilute acid leaches of mainstem samples (Galy et al., 1999; Bickle et al., 2015; Fig. 8A). This calcite to dolomite ratio is higher in these mainstem samples than in the bedloads from small tributaries which have Mg/Ca ratios in the leach fractions between 0.5 and 0.8 indicating that the carbonate is 50–80 mol percent dolomite (Fig. 8A, Electronic annex: Table E2). It is probable that calcite weathers faster than dolomite reducing the fraction of calcite in the bedloads of the small tributaries dominated by more weathered floodplain sediments. The acetic acid leaches exhibit a correlation between $^{87}Sr/^{86}Sr$ ratios and Mg/Ca ratio (Fig. 8A) which implies variable mixtures of dolomite and calcite in the floodplain bedloads with the dolomite component having an $^{87}Sr/^{86}Sr$ ratio of ~ 0.75, consistent with derivation from Lesser Himalayan dolomites (e.g. Bickle et al., 2001). The 1000Sr/Ca molar ratio of the acetic acid leaches is relatively constant at $\sim$0.5. The exceptions are leaches with low masses of Ca indicating that the bedload sample contained little carbonate and the leach Al and Na contents indicate significant contamination by silicate-derived components.

5.4.1. Calculation of carbonate and silicate inputs based on $^{87}Sr/^{86}Sr$ ratios

To calculate the magnitude of precipitation of secondary calcite we assume that carbonate dissolution of carbonate dominates the inputs of Ca to the floodplain waters (justified below). The mass of Ca derived from carbonate is calculated by first using mass balance of Sr-isotopic compositions to estimate the mass of Sr derived from carbonate and then using the relatively well constrained carbonate Sr/Ca ratio from the acetic acid leaches of mainstem bedloads to calculate the carbonate Ca input to the waters. As discussed below, the water Sr concentration also has to be corrected for precipitation of secondary carbonate and an estimate is made of the silicate Ca input to the waters. It is shown that the estimates of Ca lost to secondary carbonate are relatively insensitive to these parts of the calculation.

The fractions of silicate (F^{Sr}_{sil}) and carbonate (F^{Sr}_{crb}) Sr input into each flood plain water sample are calculated from mass balance of $^{87}Sr/^{86}Sr$ ratios as

$$\frac{^{87}Sr}{^{86}Sr_W} = F^{sil}_{Sr}.\frac{^{87}Sr}{^{86}Sr_{sil}} + F^{crb}_{Sr}.\frac{^{87}Sr}{^{86}Sr_{crb}} \quad (1)$$

where $F^{sil}_{Sr} + F^{Crb}_{Sr} = 1$ and $^{87}Sr/^{86}Sr_j$ are the Sr-isotopic compositions with $j = W$ the water sample, *sil* the silicate input, or *crb* the carbonate input. The Ca input from carbonate for each water sample can then be calculated from knowledge of the concentration of Sr in the water and an estimate of the carbonate Sr/Ca ratios from acetic acid leaches of the bedload. The measured Sr concentration will also have been reduced by precipitation of secondary carbonate but even if this smaller reduction is ignored, the calculated Ca inputs from carbonate are, on average, double the measured water Ca concentrations implying loss of ~50% of the Ca to secondary carbonate. The loss of 50% or more of Ca from the water to secondary calcite is significant to calculating the chemical weathering fluxes in the flood plain but the magnitude is consistent with the ubiquity of secondary carbonate cements in flood plain sediments (e.g. Pal et al., 2003).

Calculation of the total Ca loss also requires an estimate of the Ca input from silicate minerals which is based on water Na concentrations (corrected for saline inputs) and the Na/Ca ratio of the silicate input, although the calculations are relatively insensitive to these parameters. Correction for Sr loss to secondary carbonate requires simultaneous solution of the mass-balance equations for both Sr and Ca. The measured Sr concentration in the water (Sr_W) may be related to that prior to precipitation of secondary calcite (Sr_0) assuming Rayleigh fractionation (see for example Bickle et al., 2015) by

$$Sr_W = Sr_0\gamma^{K^{Sr}_d}, \quad (2)$$

where γ is the fraction of Ca remaining after precipitation of secondary calcite and K^{Sr}_d is the Sr/Ca molar partition coefficient for Sr into secondary calcite which is estimated as 0.05 (Bickle et al., 2015).

Solving Eqs. (1) and (2) gives the fraction of Ca remaining in the water after precipitation of secondary calcite, γ, as

$$\gamma = \frac{Ca_W}{\frac{Sr^{crb}_W.\gamma^{-K^{Sr}_d}}{Sr/Ca^{crb}} + Ca^{sil}_0} \quad (3)$$

where Ca_W is measured water Ca concentration and $Sr^{crb}_W = F^{crb}_{Sr}\,Sr_W$ is the mass of Sr in the water derived from carbonate after precipitation of secondary carbonate calculated from Eq. (1) and the measured Sr content of the water. Sr/Ca^{crb} is the Sr/Ca ratio of the carbonate input and Ca^{sil}_0 is the water Ca concentration derived from silicate before precipitation of secondary calcite calculated from the estimate of the silicate Na/Ca ratio and the measured water Na concentration corrected for saline inputs.

The composition of the carbonate inputs is best constrained by acetic acid leaches of the mainstem bedloads as floodplain tributary bedloads are thought to have lost calcite by weathering decreasing carbonate Ca and increasing their dolomite to calcite ratios (Fig. 8). The $^{87}Sr/^{86}Sr$ ratio (0.7203 ± 0.0010, 1 standard error, range 0.7183–0.7227) and the 1000Sr/Ca ratio (0.544 ± 0.061, range 0.40–0.65) of the carbonate input are therefore taken from the average of acetic acid leaches of the three Ganga mainstem bedloads collected at Rajshahi just downstream of Farakka (Galy et al., 1999) and one sample from Rishikesh where the headwaters of the Ganga enter the floodplain (Bickle et al., 2015). The $^{87}Sr/^{86}Sr$ ratios of silicate residues from leaching of the West Kosi floodplain bedloads range from 0.7585 to 0.8038 and their Na/Ca ratios from 2.1 to

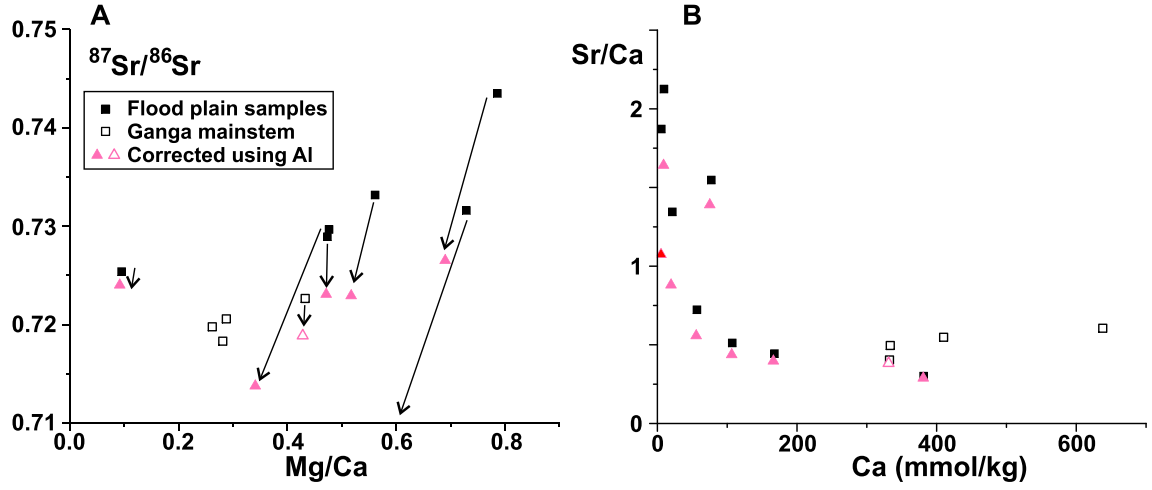

Fig. 8. (A) $^{87}Sr/^{86}Sr$ ratios versus Mg/Ca molar ratios of leaches of West Kosi flood plain samples and mainstem samples from the Ganga and (B) Sr/Ca ratio versus Ca of leaches (mmol Ca per kg of bedload sample leached). Red triangles represent compositions of dilute acid leaches corrected for potential inputs from silicate minerals on the basis of their Al concentrations and assuming silicate input has element/Al ratios of silicate residues. Lines in (A) join uncorrected and corrected compositions. Data in Electronic Annex Table E2 with Ganga downstream mainstem bedload samples from Rajshahi (Galy et al., 1999) and the Ganga where it enters the floodplain at Rishikesh (Bickle et al., 2015).

6.8 with no significant correlation. The Na/Ca ratios of the silicate residues from leaching of bed loads of the Ganga at Rishikesh average 2.6 (Bickle et al., 2015). The Na/Ca ratios of the silicate fraction of the suspended load of the mountain rivers sampled by Lupker et al. (2012a) average 3.5. The silicate fractions of the suspended loads of the Ganga in Bangladesh (where total Ca is corrected for the quoted carbonate contents) averages 2.3 with no significant variation with depth (Lupker et al., 2012a). The higher mean Na/Ca ratio of 5.1 for the silicate residues of the bed loads from the floodplain rivers may reflect their more weathered nature. This suggests that Ca is more easily leached than Na and that the Na/Ca ratio of the silicate inputs is lower than that of the parent silicate material.

For the mean $^{87}Sr/^{86}Sr$ and Sr/Ca ratios of carbonate given above and a best estimate of the silicate $^{87}Sr/^{86}Sr$ of 0.75 (discussed below) and silicate Na/Ca ratio of 2.5, the loss of Ca to secondary carbonate (γ) for the West Kosi flood plain tributaries ranges from 0.14 to 0.91 (Fig. 9). The suite of high Na/Ca water samples from the Gomti catchment have consistently low γ values (0.14–0.23) presumably attesting to waters which have undergone a combination of extensive evaporative loss and redissolution of the precipitated salts and these 6 samples are excluded from the quoted averages. Without these samples the mean γ value is 0.48. The calculated values of γ are most sensitive to the uncertainties in the carbonate 1000Sr/Ca ratio and the silicate $^{87}Sr/^{86}Sr$ ratio. The range of 0.40–0.65 in the carbonate 1000Sr/Ca ratio gives a range in the calculated average γ values (0.36–0.57). Increasing the silicate $^{87}Sr/^{86}Sr$ ratio from 0.750 to 0.775 decreases the average γ value from 0.48 to 0.38. The uncertainties in the other parameters have limited impact on the calculated γ values (see Electronic annex: Table E6). The uncertainty in carbonate Sr/Ca ratios therefore dominates the overall uncertainty in γ. However given the assumptions in the calculations and the potential heterogeneities of the inputs discussed below we would caution against over confidence in the significance of these results.

5.4.2. Incongruent dissolution, heterogeneity and $^{87}Sr/^{86}Sr$ ratios of silicate inputs

The solution of Eqs. (1)–(3) also predicts the silicate input Sr/Ca ratio as a function of the assumed silicate Na/Ca ratio and $^{87}Sr/^{86}Sr$ ratio (Fig. 10). The array of calculated silicate Sr/Ca ratios as a function of assumed Na/Ca ratios calculated for the average silicate $^{87}Sr/^{86}Sr$ ratio of 0.779 lies well below the measured Sr/Ca ratio in the silicate residues from leaching for the flood plain bedload samples, mountain river bedload samples and the bed load from the Ganga at Rishikesh (Bickle et al., 2015). Decreasing the assumed silicate $^{87}Sr/^{86}Sr$ ratio increases the calculated Sr/Ca ratios reducing the discrepancy.

It is probable that dissolution of the silicate minerals is incongruent. Plagioclase, with lower $^{87}Sr/^{86}Sr$ and Sr/Ca ratios, is likely to weather faster than higher $^{87}Sr/^{86}Sr$ ratio white micas. Garçon et al. (2014) present analyses of Sr concentrations and $^{87}Sr/^{86}Sr$ ratios of minerals separated from bedload collected from the Ganga mainstem at Hardinge Bridge in which the $^{87}Sr/^{86}Sr$ ratio of plagioclase is 0.7227, K-feldspar 0.7587, epidote 0.7125, muscovite 0.831 and biotite 0.812. The low $^{87}Sr/^{86}Sr$ ratio and high $^{143}Nd/^{144}Nd$ ratios of the epidote coupled with the very low $^{87}Sr/^{86}Sr$ ratio of carbonate in the sample (0.7139) probably reflect bedload additions from the southern tributaries. These are dominated by mafic inputs from the low $^{87}Sr/^{86}Sr$ ratio Deccan lavas and low $^{87}Sr/^{86}Sr$ ratio carbonate from the Vindhyan sequence (Ray et al., 2003). An input from the southern rivers is consistent with the lower $^{206}Pb/^{204}Pb$ ratios of the plagioclase and epidote compared to the K-feldspar (Garçon et al., 2013). Lupker et al. (2012a) report that the Ganga suspended loads reflect significant time-dependant inputs from the southern rivers. However K-feldspar is likely to be predominantly Himalayan-derived and by implication Himalayan-derived plagioclase is unlikely to be much less radiogenic. Sr-isotopic mineral heterogeneity of the silicate detrital load is also confirmed by the analyses of the whole silicate fractions of three suspended samples and three bedloads from the downstream Ganga where the silicate fractions of the bedloads range from 0.7546 to 0.7589 but the mica-enriched suspended loads range from 0.768 to 0.774 (Garçon et al., 2014). The West Kosi floodplain tributaries have $^{87}Sr/^{86}Sr$ ratios up to 0.7365 putting a minimum limit on the silicate input $^{87}Sr/^{86}Sr$ ratios. We infer that $^{87}Sr/^{86}Sr$ ratios of the silicate inputs are most likely to be in the range 0.75–0.76.

The second implication of the calculated silicate Sr/Ca ratios is that silicate fractions of the bedloads are heterogeneous. This is consistent with the observation that both the silicate residues of bedloads sampled in mountain rivers and those from the floodplain exhibit a wide range of Na/Ca ratios which correlate with their Sr/Ca ratios (Fig. 10). It seems probable that this correlation is a consequence of a single control on the silicate Ca concentration such as the proportion of Ca-plagioclase in the sample. However there is no significant correlation between the $^{87}Sr/^{86}Sr$ ratio and Na/Ca ratio of the silicate residues. The calculated silicate

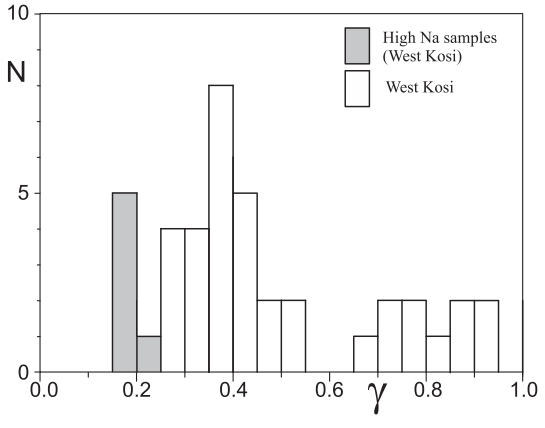

Fig. 9. Histogram of fraction of Ca remaining in West Kosi flood plain samples (γ) calculated from equation 3 assuming 1000Sr/Ca of carbonate input equals 0.544, and Na/Ca of the silicate input equals 2.5, and silicate $^{87}Sr/^{86}Sr = 0.75$. Grey boxes are γ values for samples with high Na/Ca ratios mainly from the Gomti catchment.

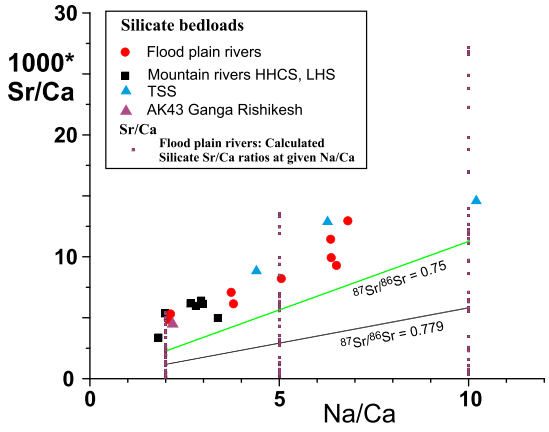

Fig. 10. Lines illustrate the variation of the calculated mean silicate input Sr/Ca ratios of the 41 flood plain water samples calculated from Eqs. (1) and (3) plotted for the given silicate $^{87}Sr/^{86}Sr$ ratio against the assumed silicate Na/Ca ratio. Small squares show the individual Sr/Ca values of the flood plain waters calculated for silicate Na/Ca ratios of 2.0, 5.0 and 10.0 for a silicate $^{87}Sr/^{86}Sr$ ratio of 0.75. Coloured symbols are the compositions of bedload silicate residues (Electronic annex Table E2, key on figure) excluding the very high Na/Ca bedloads from the Marsyandi catchment).

Sr/Ca ratios at any chosen Na/Ca ratio exhibit a wider dispersion then the silicate fractions of the bedload samples (Fig. 10) which increases at high Na/Ca ratios. This apparent dispersion must reflect heterogeneity in the inputs of silicate Na/Ca, Sr/Ca and $^{87}Sr/^{86}Sr$ ratios where weathering of more altered plagioclase-poor and mica-rich silicate residues inputs a component with higher $^{87}Sr/^{86}Sr$, Sr/Ca and Na/Ca ratios.

5.4.3. Calculation of fractions of Ca, Sr and Mg derived from carbonate and silicate: West Kosi

The fractions of Sr and Ca derived from silicate and carbonate sources in the West Kosi samples are calculated from Eqs. (1) and (3), with the correction for loss to secondary calcite. Excluding the high Na/Ca samples, the results indicate that between 1.7 and 22% of the Ca (mean 8.4%) and 1.4–55% of the Sr (mean 31%) are derived from silicate sources (Fig. 11A and B, Electronic Annex: Table E6). These values are calculated for parameter values with carbonate Sr/Ca (0.544) and silicate Na/Ca (2.5) in the centre of their probable range. The $^{87}Sr/^{86}Sr$ ratio of silicate is taken as 0.75 as discussed above. The estimated average fraction of silicate Sr (~31%) is in the same range as estimates of the fraction of silicate Sr in the mountain rivers (25–35% Galy et al., 1999; 24% Jacobson et al., 2002; 33% Bickle et al., 2015).

The Sr-isotopic compositions put no constraints on the relative fractions of Mg derived from carbonate and silicate sources. The Mg/Ca ratios of the carbonate leach are variable and indicate mixed calcite-dolomite mineralogies with calcite likely to weather faster than dolomite. However the Na/Mg ratios of the floodplain and mountain river bedload silicate residues are relatively constant at 1.91 ± 0.20 and 1.89 ± 0.28 (1 standard error) respectively. We therefore estimate the fraction of silicate Mg from the water Na concentration corrected for saline inputs and calculate the carbonate Mg input by difference. This indicates that the fraction of silicate-derived Mg ranges from 16 to 96% (mean 45%). This excludes the samples from the Gomti catchment for which the calculation implies silicate Mg input about double that of the water composition.

The calculations also allow estimates of the input carbonate Mg/Ca ratios and, as for the input silicate Sr/Ca ratios discussed above, they vary over a wide range (Fig. 11D). The mean calculated carbonate Mg/Ca ratio is ~0.16 which compares with 0.52 for the acetic acid leaches of the flood plain bedloads and reflects the faster dissolution rate of calcite compared to dolomite which makes up ~40% of the carbonate in the suspended loads (Galy et al., 1999; Garzanti et al., 2010, 2011; Lupker et al., 2012a).

5.4.4. Calculation of fractions of Ca, Sr and Mg derived from carbonate and silicate: East Kosi

The water samples from the East Kosi scatter about the line defined by the acetic leaches and residues on plots of Sr/Ca versus Na/Ca (Fig. 7) and Mg/Ca versus Na/Ca (Electronic Annex Fig. E2). There is no systematic displacement of the water samples to high Sr/Ca and Mg/Ca as expected from loss of secondary calcite although this is likely obscured by the scatter. The water samples all have $^{87}Sr/^{86}Sr$ ratios lower than both the leaches and residues of the two bedload samples analysed. It is probable, from their high $^{87}Sr/^{86}Sr$ ratios that these bedloads are dominated by detritus from the Lesser Himalayas but that the waters derive much of their cation load from the less radiogenic High Himalayas and Tibetan Sedimentary Series. The fractions of silicate and carbonate-derived cations have been calculated as in Bickle et al. (2015), Eq. (4), from the set of mass balance equations for Sr, Ca and Na or Mg, Ca, Na (loss to secondary calcite could not be resolved)

$$X^i_{Cwat} = F_{crb}X^i_{crb} + F_{sil}X^i_{sil} \quad (4)$$

where X^i_{Cwat} (μmol/L or nmol/L) is the concentration of the cation, i, in the water, F_{crb} and F_{sil} the weight fractions (g/L) of carbonate and silicate input and X^i_{crb} and X^i_{sil} the concentrations of cations in the carbonate and silicate inputs (mmol/kg or μmol/kg). The regressions are carried out with the acetic acid leach compositions of sample AK388 for the composition of the carbonate input as the acetic acid leach of AK401 has very low Ca and the little carbonate leached is likely to be contaminated by silicate. Using the residue cation ratios of AK388 (Na/Ca = 6.4, Sr/Ca = 11.4) or AK401 (Na/Ca = 3.8, Sr/Ca = 6.1) regression of Sr—Ca—Na gives average percentage silicate Sr of ~71% (range 47–95%) and average percentage silicate Mg of ~55% (range 9%–65%) for the set of 15 out of 18 East Kosi flood plain water samples (Electronic Annex Table E7). The calculated average percentage silicate Ca input is directly proportional to the assumed silicate Na/Ca ratio and thus varies from 15% using the Na/Ca ratio of AK388 to 26% using that of AK401. The insensitivity of the fractions of silicate Sr and Mg to the choice of silicate

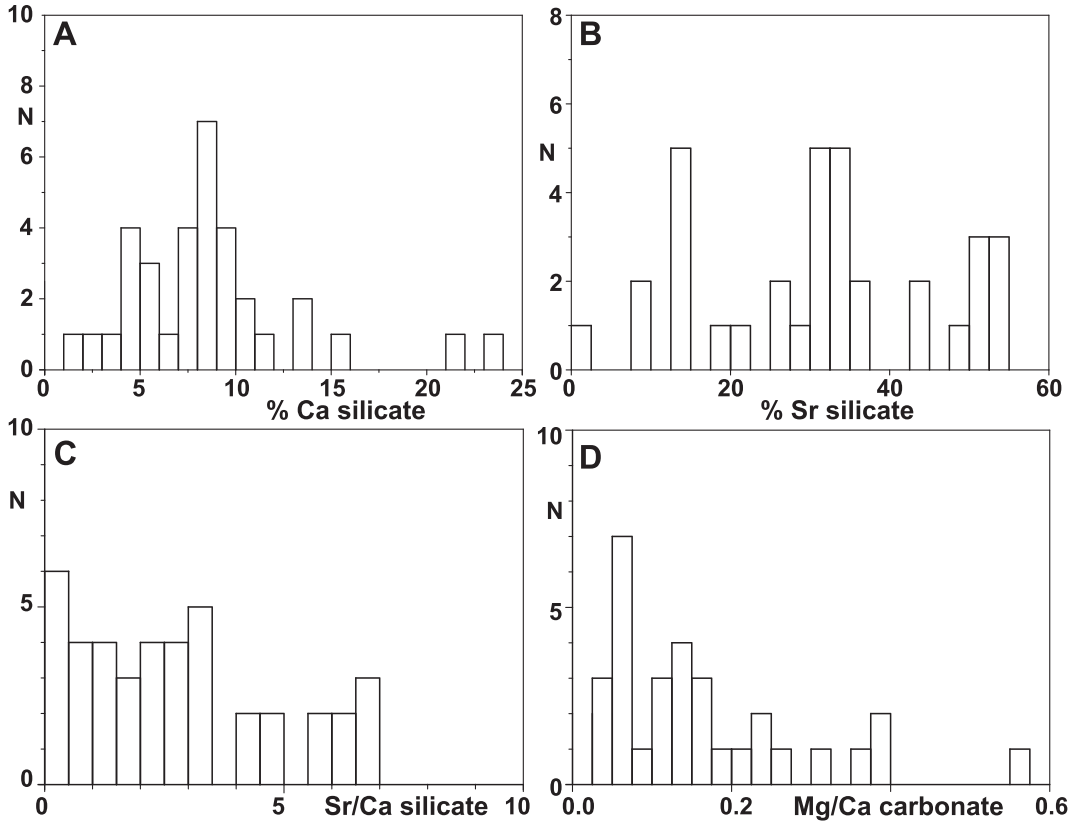

Fig. 11. Histograms of (A) the distribution of percentage of Ca, (B) Sr derived from silicates in the West Kosi flood plain tributaries, (C) the Sr/Ca ratio of silicate inputs and (D) the Mg/Ca ratio of carbonate inputs calculated for flood plain tributaries. Calculated from Eqs. (1) and (3) assuming silicate $^{87}Sr/^{86}Sr = 0.75$, silicate Na/Ca = 2.5, carbonate 1000Sr/Ca = 0.545 and $^{87}Sr/^{86}Sr = 0.7203$ and silicate Na/Mg = 1.91.

residue compositions is expected, as discussed by Bickle et al. (2005). Calculations in Mg-Ca-Na space give similar values (Electronic Annex: Table E7) and the average of all four regressions has been used.

The output fluxes from the floodplain from salt, carbonate and silicate sources combined by weighting by the areas of the West Kosi and East Kosi floodplains are listed in Electronic Annex E10.

6. THE MAGNITUDE OF CHEMICAL WEATHERING ON THE FLOOD PLAIN

The magnitude of chemical weathering on the Ganga flood plain may be estimated in two ways, (1) by subtraction of the weathering fluxes input by rivers from the Himalayas to the north and from the Deccan plateau to the south from the discharge at Farakka or (2) by mass balance of the conservative chemical and isotopic components, where the chemistry of the input from the flood plain is taken as the average of the flood plain tributaries. A compilation of the chemistries and chemical fluxes carried by the major rivers from the Himalayas to the north and Deccan plateau to the south and the deconvolution of these fluxes into contributions from salts (rain, evaporate and springs), carbonate and silicate minerals is presented below.

6.1. Chemical inputs by Himalayan Rivers

The seven major rivers which enter the Ganga flood plain from the Himalayas are from west to east: Yamuna, Alaknanda and Bhagirathi (which combine to form the Ganga), Sarda, Karnali, Rapti, Narayani in Nepal or Gandak in India and the Kosi (Fig. 1). The Sarda and Karnali combine on the flood plain to form the Ghaghara which is joined by the Rapti before the Ghaghara joins the Ganga just above Patna. The Yamuna flows ~800 km across the flood plain before joining the Ganga at Allahabad. The chemical and isotopic sampling of these rivers at the edge of the flood plain is variable. The Ganga at Rishikesh, 25 km north of Haridwar, was sampled nearly every month for 2½ years after May 1996 (Bickle et al., 2003), data supplemented (see Electronic annex: Calculation of chemical fluxes) by a few other samples (Sarin et al., 1989; Bickle et al., 2005, 2015; Rai et al., 2010) (see Electronic annex: Calculation of chemical fluxes). Relatively few published analyses are available from the Yamuna and the Nepalese rivers (five samples from the Yamuna, four samples from the Narayani, one from the Rapti and Karnali and none from the mainstem Kosi in Nepal. These samples of the Nepalese rivers have been supplemented by collections in 2015 and 2016 reported in this paper. No analyses are avail-

able for the Sarda in western Nepal. Given the very variable densities of sample collection and availability of discharge data for each of the major Himalayan rivers, the methods for estimating the discharge-weighted chemical fluxes and their uncertainties have been tailored to the available data (see Electronic annex: Calculation of chemical fluxes).

6.1.1. Seasonal variability and calculation of the mean chemical fluxes of the Ganga at Rishikesh

Water discharge in the Ganga from the mountains during the monsoon months (July to September) is ~ 65% of the annual flux (Pal, 1986). The chemical and Sr-isotopic composition varies with the discharge. Concentrations of Na, K, Ca, Mg, Si and Sr exhibit increases of between a factor of 1.4 (K, Ca) to ~3.0 (Na, Cl) between the wet and dry seasons (Fig. 12). The element ratios to Ca also exhibit systematic variations with Na/Ca, Mg/Ca and Sr/Ca all exhibiting marked decreases at high discharge (Fig. 13). These changes are predominantly the consequence of changes in the relative magnitudes of the discharge from the geologically distinct catchments feeding the river (e.g. Bickle et al., 2003) combined with seasonal changes in weathering mechanisms (e.g. Tipper et al., 2006; Bickle et al., 2015).

The discharge weighted mean for the Ganga at Rishikesh (Table 2, Electronic annex: Calculation of chemical fluxes) has been calculated from the monthly averages of the chemistry multiplied by the monthly discharge in the Ganga in 1972 just downstream of Devprayag (50 km upstream of Haridwar) (Pal, 1986).

6.1.2. Yamuna chemical fluxes

Chemical and Sr-isotopic data for the Yamuna is available for the pre-Monsoon (June 1999), monsoon (September 1999) and post-monsoon (October 1998) from Dalai et al. (2002, 2003) and chemical data for March and November, 1983, from Sarin et al. (1989). The discharge weighted mean of the Yamuna is calculated by partitioning the chemistry between monsoon months (July, August and September) and dry season months (October to June) (Electronic annex: Calculation of chemical fluxes).

6.1.3. Nepalese rivers chemical fluxes

Extensive discharge data is collected for the Nepalese rivers by the Department of Hydrology and Meteorology, Kathmandu and monthly discharge data for the Karnali (1962–1993), Rapti (1964–1985), Narayani (1963–1993) and Kosi (1977–1985) has been obtained from the Global Runoff Data Centre, 56068 Koblenz, Germany.

The chemical discharge-weighted mean of the Narayani is based on nine samples, five from France-Lanord et al. (2003) with $^{87}Sr/^{86}Sr$ the average of values given by Galy et al. (1999) and averages of four sets of samples collected over short periods in July and September 2015 and June and August 2016, as part of this study (Electronic annex: Table E1). Discharge-weighted chemical fluxes have been calculated by regressing the chemical concentrations against average monthly discharges (Electronic annex: Calculation of chemical fluxes).

There are only single published analyses of the Rapti and Karnali on samples collected in November at low flow (Galy and France-Lanord, 1999; Galy et al., 1999) and these have been combined with the averages of single sets of samples from this study collected in July 2015. The discharge-weighted mean concentrations of these rivers have been calculated assuming that the November sample of Galy and France-Lanord (1999) is characteristic of the dry season months November to May and the July sample from this study the monsoon season June to October.

There are no published analyses of the Kosi below the confluence of the Arun and the Sun Kosi. We use the average of three sample sets collected for this study in July 2015 and June and August 2016. These were all collected during the monsoon and their average concentration has been increased by a factor of 1.1, the difference in mean concentration for the Ganga at Rishikesh June to September cations compared to flux-weighted annual averages. The Sarda in West Nepal (Fig. 1) has no reported analyses and we assume it has the same chemical and Sr-isotopic composition as the next major river to the East, the Karnali.

6.1.4. Discharge-weighed mean inputs from the mountains

The mean discharge-weighted chemical inputs to the flood plain from the Himalayas have then been calculated by summing the discharge-weighted chemistries of the seven Himalayan rivers given the estimates of their annual discharges given in Table 2. The uncertainties on this weighted average were calculated by the same Monte-Carlo routine as for the Ganga at Rishikesh and Farakka. The uncertainties on the discharge-weighted mean chemistries of the Ganga at Rishikesh and the Narayani were calculated as given in Electronic annex: Calculation of chemical fluxes. The 1σ uncertainty on each element concentration in the other six rivers is taken as 15% and the uncertainty on a single $^{87}Sr/^{86}Sr$ analysis of 0.003 based on the average estimate of the uncertainty on a single sample from the Alaknanda data (i.e. using Electronic Annex: equation E6). An arbitrary uncertainty of 20% has been assigned to the poorly constrained discharge of the Yamuna, Ganga and Sarda with the uncertainties on a single year annual discharge of the other Nepalese rivers calculated from the monthly discharge data. The mean and 1σ uncertainties on the mean chemical compositions and discharges to the flood plain are given in Table 2 and their element ratios illustrated in Fig. 14. The spread in compositions caused by differences in relative inputs from the distinct geological terrains is small given the uncertainties. The Kosi exhibits the highest Na/Ca ratio, the Ganga and Kosi the highest $^{87}Sr/^{86}Sr$ ratios and the Yamuna the lowest $^{87}Sr/^{86}Sr$ ratio.

6.1.5. Calculation of fractions of Sr, Ca and Mg derived from salts, carbonate and silicate: Himalayan rivers

The estimates of the fractions of Sr, Ca and Mg derived from salts, carbonate and silicate minerals for the Himalayan rivers are based on the calculations for the Marsyandi draining the Tibetan sedimentary series in Nepal, the High Himalayan Rishi Ganga catchment and the three lesser

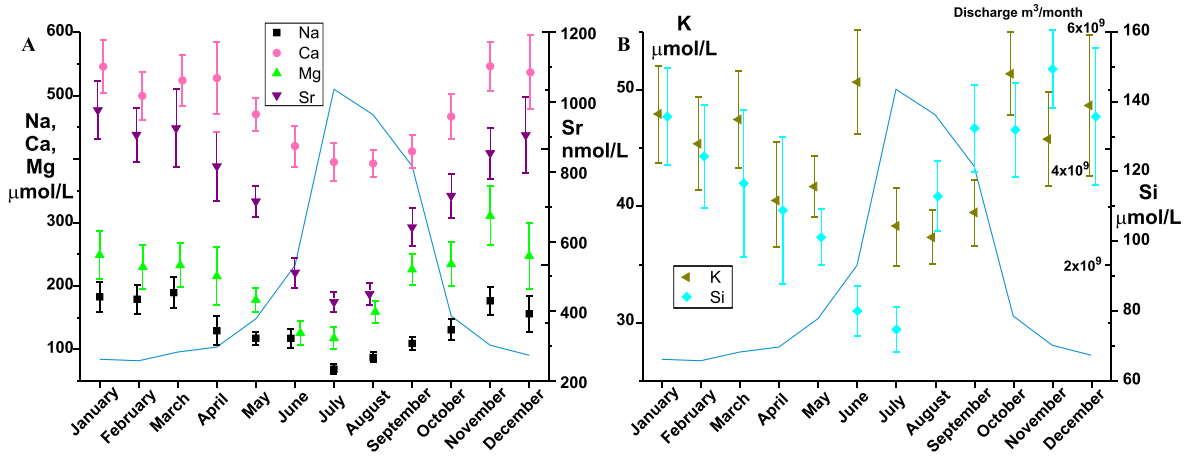

Fig. 12. Average monthly concentrations in the Ganga at Rishikesh with 1 x standard errors. (A) Na, Ca, Mg and Sr. (B). Average monthly K and Si concentrations. Note systematic change in all elements. Blue line shows monthly discharge in 1972 from Pal (1986) with values shown inside right axis on Fig. 12B. Error bars calculated as described in the Electronic Annex: Calculation of chemical fluxes (Eqs. (E1)–(E3)).

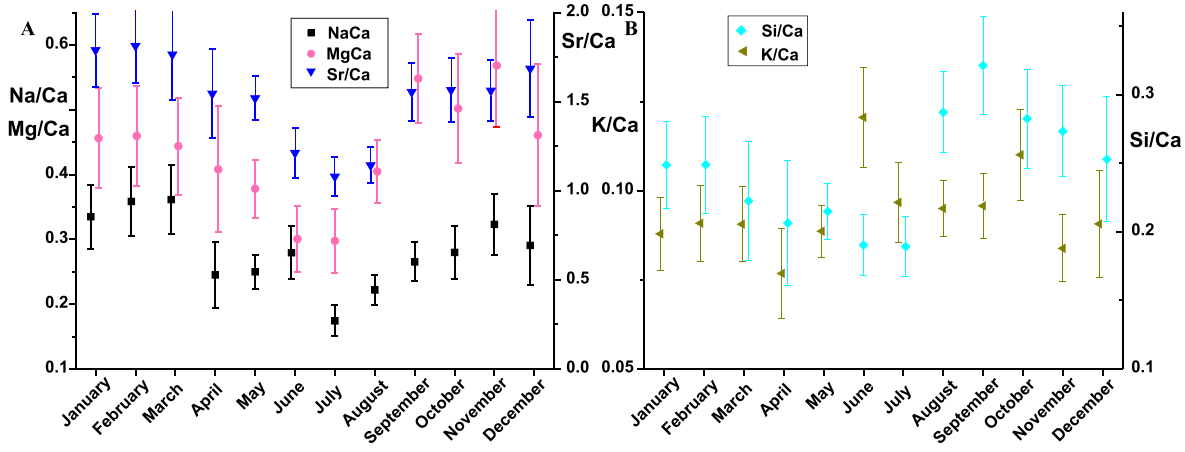

Fig. 13. Average monthly element to Ca ratios for the Ganga at Rishikesh with 1 x standard errors.

Himalayan catchments presented by Bickle et al. (2015). The fractions have been weighted by the mean annual relative inputs from each of the three litho-tectonic units given by Bickle et al. (2003) and the mean of these applied to the mean discharge of the Himalayan rivers (Table 2). The results summarised in Electronic Annex, Table E8.

6.2. Inputs by the Southern rivers

There are six large tributaries which join the Ganga from the south (Fig. 1). The Chambal and the Betwa drain into the Yamuna. The Kunwari joins the Sindh before draining into the Yamuna. The Ken, Tons and the Son drain into the Ganga below its confluence with the Yamuna. The Chambal, Kunwari, Betwa, Tons and Son were sampled at high flow in August 2003 for this study. Analyses of samples of the Chambal and Son collected in March and September, 1982 and November 1983, and the Ken and Betwa collected in March 1982 and November 1983, were published by Sarin et al. (1989) and Krishnaswami et al. (1992).

The mean compositions of the southern rivers exhibit a limited dispersion in Na/Ca ratios (0.5–1.5) positively correlated with Sr/Ca and Mg/Ca ratios (Fig. 15). The Son has a higher $^{87}Sr/^{86}Sr$ ratio (0.725) compared with the other southern rivers ($^{87}Sr/^{86}Sr$ ratios between 0.712 and 0.714). The Son and the Tons primarily drain the Proterozoic Vindhyan sequences (Ray et al., 2003; McKenzie et al., 2011). The Ken drains the predominantly gneissic or granitoid Archaean Bhundelkhand massif (Mondal et al., 2002) as well as the Vindhyan sequence. The Betwa, Sindh and the Kunwari drain the Bhundelkhand massif with the headwaters extending into the Deccan basalts. The Chambal and its tributaries drain extensive areas of the Deccan traps. Most of the lavas in the Deccan traps have $^{87}Sr/^{86}Sr$ ratios of ~0.705 although some of the lowest formations, extensively contaminated by continental crust, exhibit $^{87}Sr/^{86}Sr$ ratios of ~0.715 (e.g. Cox and Hawkesworth, 1985). Dessert et al. (2001) measured $^{87}Sr/^{86}Sr$ ratios between 0.708 and 0.715 on rivers draining the Deccan basalts, values possibly elevated by inputs from adjacent Precambrian gneissic crust.

Table 2
Mean chemical compositions of Himalayan rivers entering floodplain and discharge-weighted mean.

River	Na	K	Ca	Mg	Si	Cl	SO_4	Sr	$^{87}Sr/^{86}Sr$	Discharge[g]	
	μmol/L							nmol/L		10^9 m^3/yr	1σ
Yamuna[d]	166	62	665	284	164	39	223	1135	0.72644	10.5	2.1
Sapt Kosi[b]	92	42	345	79	125	20	109	371	0.75084	48.8	3.9
Rapti[b]	121	69	900	389	143	16	127	1096	0.73609	3.9	1.0
Karnali[b]	91	41	610	235	94	7	116	1010	0.72670	43.7	7.0
Sarda[a,c]	91	41	610	235	94	7	116	1010	0.72670	23.0	3.7
Alaknanda[e]	99	41	422	168	107	23	144	572	0.73923	22.4	4.5
1σ Alaknanda	5	1	12	9	4	2	5	20	0.00069		
Narayani[b]	112	60	610	258	104	47	164	934	0.73486	49.5	5.6
1σ Narayani	10	2	57	23	10	5	16	84	0.00036		
Mean[f]	102	49	533	201	110	24	135	797	0.73301	202.0	
1σ Mean[f]	5	2	28	11	6	2	7	45	0.00121	12.7	

[a] Sarda taken as same composition as Karnali.
[b] Discharge from Global Runoff Data Centre files (Fekete et al., 2000) sent 11/04/2016 http://www.bafg.de/GRDC/EN/Home/homepage_node.html.
[c] Discharge from Wikipedia http://en.wikipedia.org/wiki/Sharda_River accessed 5/02/2015.
[d] Discharge from Jha et al. (1988).
[e] Discharge from Pal (1986).
[f] Discharge weighted mean and 1σ uncertainties calculated by Monte Carlo routine given calculated uncertainties on mean Alaknanda and Narayani compositions (see Electronic annex: Calculation of chemical fluxes) and assuming 15% 1σ uncertainties on all other element concentrations and 0.003 on $^{87}Sr/^{86}Sr$ ratios.
[g] Standard deviation of annual discharge except 20% for Alaknanda, Yamuna and Sarda.

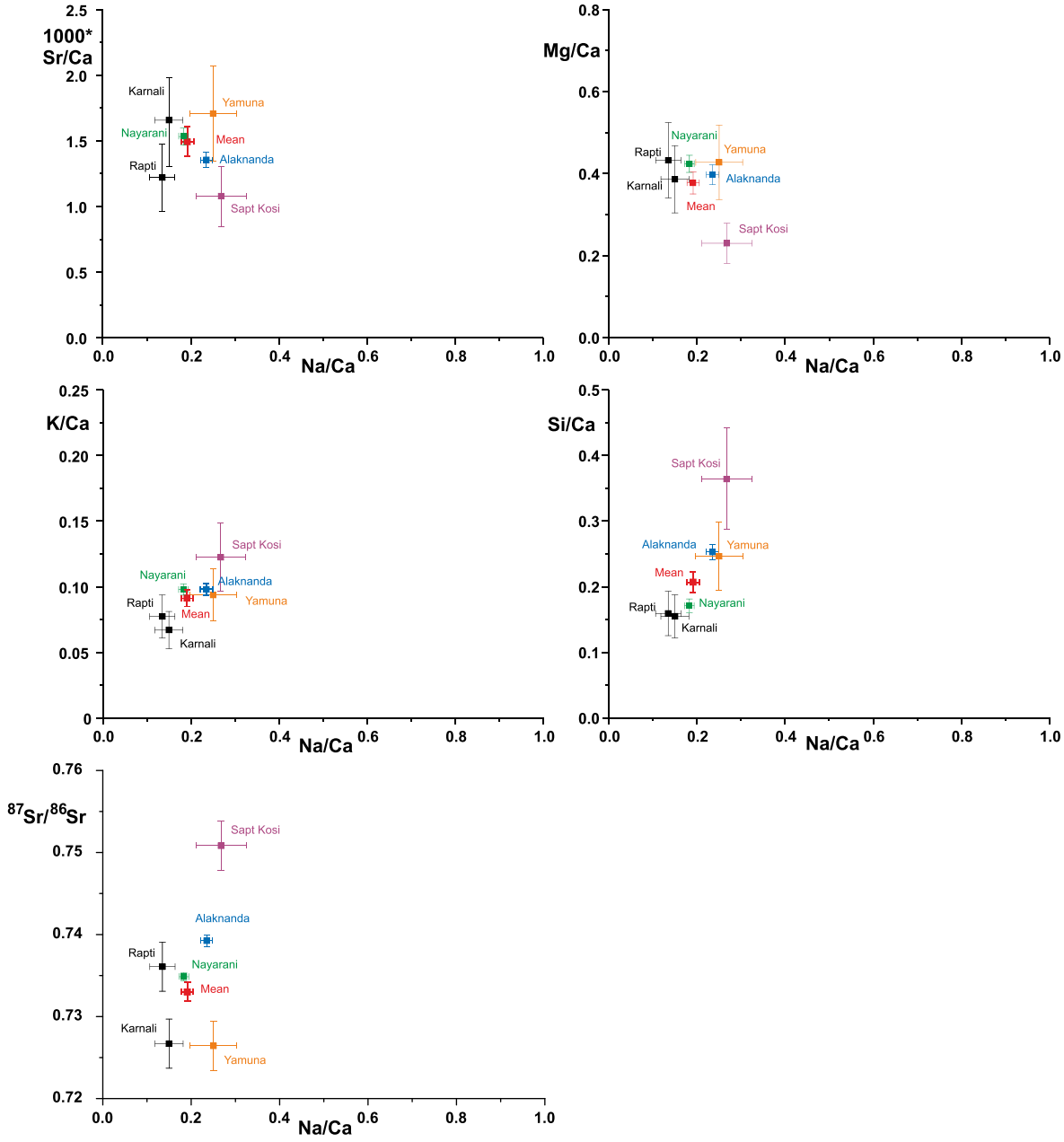

Fig. 14. Mean 1000Sr/Ca, Mg/Ca, K/Ca, Si/Ca and $^{87}Sr/^{86}Sr$ ratios of major rivers entering the flood plain from the Himalayas and discharge-weighted mean with error bars representing 1 standard error on mean calculated as described in text.

The discharge-weighted means of these analyses are presented in Table 3 together with the discharge-weighted mean calculated as for the Himalayan rivers (see Electronic annex: Calculation of chemical fluxes). All the southern river catchments are dammed with a consequent increase in dry season concentrations, which might result in the means calculated in Table 3 being over estimates. These means are therefore compared with an estimate of the southern river average chemistries based on the monsoon samples (single August samples for the Tons, Ken, Betwa and Kunwari; August and September samples for the Son and Chambal) adjusted for the increased dilution during the monsoon using the factors observed in the Ganga. The August and September concentrations are increased by the same factor as the ratio of the discharge-weighted annual mean concentrations for the Ganga data at Rishikesh to the monthly values (a factor of 1.13 for August and 1.01 for September). The Na, Mg, Cl and SO_4 concentrations are about 20% lower using these adjusted summer month estimates but the K, Ca, Si, and $^{87}Sr/^{86}Sr$ are within the uncertainties (Table 3).

6.2.1. Calculation of fractions of Ca, Sr and Mg derived from salts, carbonate and silicate: Southern rivers

The only published analyses of bedloads of the southern rivers are three bedload and one surface suspended load

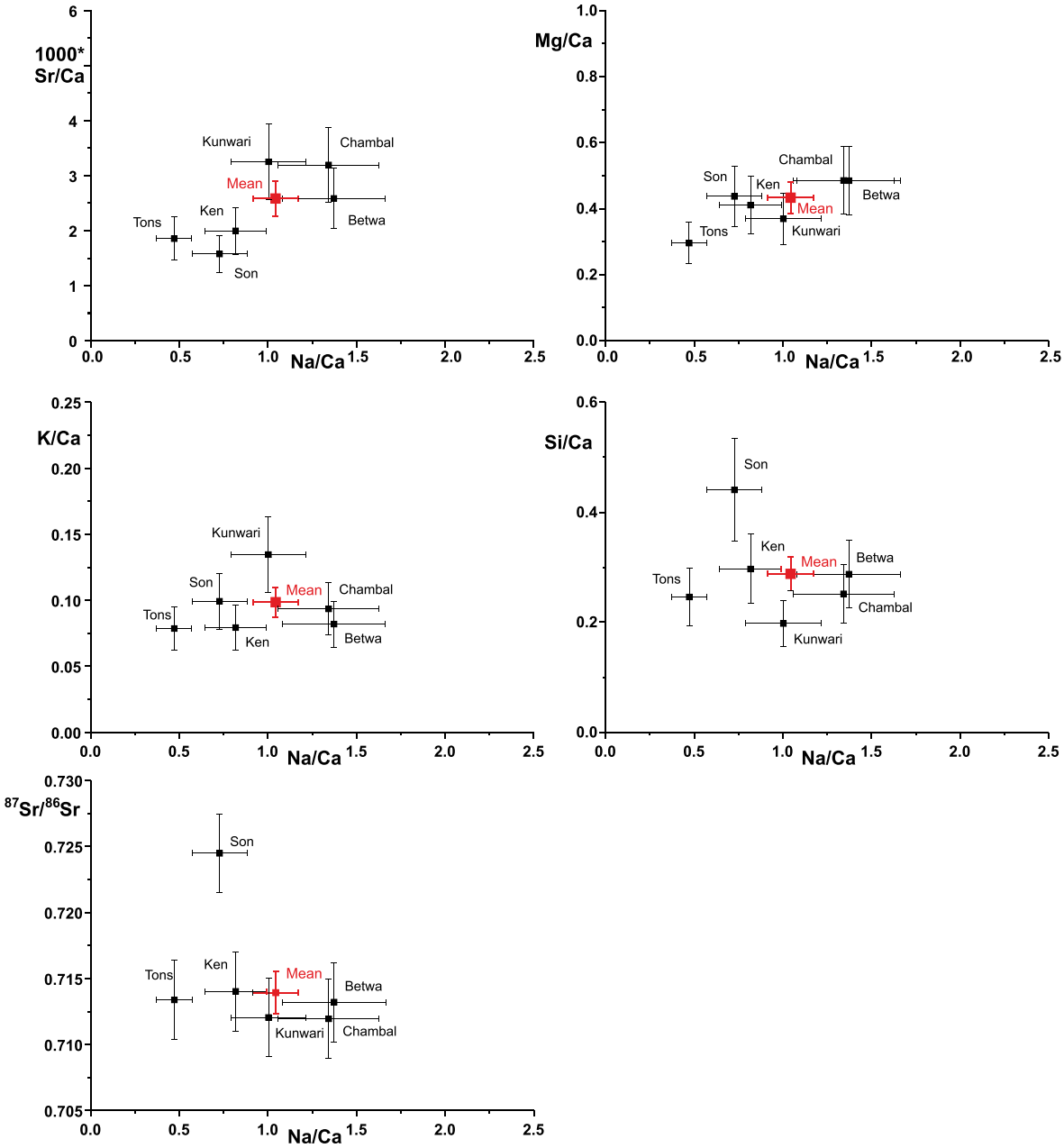

Fig. 15. Mean cation/Ca, Si/Ca and $^{87}Sr/^{86}Sr$ ratios versus Na/Ca ratios of southern rivers calculated as in Table 3.

from the Chambal (Lupker et al., 2012a). The catchments of all the southern rivers include the unmetamorphosed sandstone, shale and carbonate sequence of the mid-Proterozoic Vindahyan sequence and its older gneissic basement. The headwaters of all the rivers except the Son extend into Deccan Plateau basalts which underlie most of the catchment of the Chambal. The silicate Na/Ca ratios of the three bedload samples with carbonate fractions analysed by Lupker et al. (2012a) range from 0.7 to 1.5 and their Mg/Ca ratios from 0.6 to 1.3. The Deccan basalts have average Na/Ca ratios of 0.43 (Cox and Hawkesworth, 1985; Peng et al., 1998) but the Chambal has a mean salt-corrected Na^*/Ca^* of 1.1. Rengarajan et al. (2009), reporting similar Na/Ca ratios in tributaries to the Chambal, ascribe the high Na/Ca ratios to dissolution of Na salts in the catchment. It is probable that precipitation of secondary carbonates also elevates Na/Ca, Mg/Ca and Sr/Ca ratios in the southern rivers. The calcite-dominated carbonates in the Vindahyan sequence have a mean 1000Sr/Ca ratio of 0.68 (Ray et al., 2003). The average Mg/Ca of all the carbonate samples (dolomite and calcite) analysed is 0.13 with a slightly lower 1000Sr/Ca of 0.54.

Eqs. (5) and (6) in Bickle et al. (2015) are used to regress the average compositions of the southern rivers with either Sr—Ca—Na or Sr—Na—Ca—Mg. The input to all the rivers except the Chambal is assumed to have the silicate-derived

Table 3
Mean chemical compositions of Southern rivers entering floodplain and discharge-weighted mean.

River	No. samples	Na	K	Ca	Mg	Si	Cl	SO_4	Sr[e]	$^{87}Sr/^{86}Sr$[e]	Discharge[a]
		μmol/L							nmol/L		m^3/year
Son[b]	5	310.1	42.3	426.5	186.3	187.9	111.0	44.7	672	0.72448	3.180E+10
Tons[d]	1	305.0	50.9	647.5	191.4	159.2	89.7	72.0	1200	0.71338	5.910E+09
Betwa[c]	3	1135.6	67.8	827.4	401.1	237.8	257.1	47.2	2139	0.71321	1.000E+10
Ken[c]	3	583.5	56.6	713.5	292.8	211.8	179.5	44.8	1424	0.71403	1.130E+10
Chambal[b]	4	920.5	64.1	685.6	332.7	172.6	340.1	154.1	2190	0.71195	3.005E+10
Kunwari[d]	1	975.3	130.9	972.2	358.6	192.1	258.1	79.4	3161	0.71205	1.339E+10
Mean		687.4	64.9	658.9	285.3	189.8	218.0	83.2	1702	0.71393	
1σ Mean		65.2	5.5	50.9	22.8	13.6	21.6	10.0	163	0.00160	
Mean[f]		531.2	66.8	668.3	241.0	214.2	173.1	59.4	1666	0.71378	
1σ Mean[f]		47.1	5.5	53.5	18.7	15.6	15.7	5.0	164	0.00156	

[a] Discharges from Rao (1975) except Kunwari-Sindh catchment calculated from ratio of its catchment area to that of the Chambal.
[b] Discharge-weighted average calculated from August samples in this study for months of June to August, September sample from Sarin et al. (1989) for September and average of March and November samples from Sarin et al. (1989) (and October sample of Rai et al., 2010 for Sons) applied to months October to May where monthly discharges assumed proportional to those of the Ganga at Harding Bridge from Hossain et al. (1987).
[c] Discharge weighted average calculated with August samples in this study assigned to June to September and average of March and November samples of Sarin et al. (1989) assigned to October to May.
[d] August samples from this study with concentration increased by 13%, the difference between the Ganga at Rishikesh August sample and the discharge-weighted mean.
[e] Sr and $^{87}Sr/^{86}Sr$ data for Chambal includes data from Krishnaswami et al. (1992) and Son includes data from Krishnaswami et al. (1992) and Rai et al. (2010).
[f] Mean estimated from monsoon analyses scaled to annual mean as for Ganga at Rishikesh.

Na/Ca (2.9), 1000Sr/Ca (3) and Mg/Ca (0.24) ratios of rivers draining average silicate crust (Gaillardet et al., 1999). The silicates inputs to the Chambal are assumed to have the average Na/Ca (0.75) and Mg/Ca (0.84) ratios of the bedloads (carbonate fraction removed) from the Chambal analysed by Lupker et al. (2012a) and the average 1000Sr/Ca (1.4) of the Deccan basalts (Cox and Hawkesworth, 1985; Peng et al., 1998). The bedload Na/Ca and Mg/Ca ratios may be compared with the mean Na/Ca = 0.44, Mg/Ca = 0.84 of the Deccan basalts. The carbonate inputs to all the rivers are assumed to have the Sr/Ca and Mg/Ca of the limestones of the Vindahyan sequence (Ray et al., 2003). The calculation gives fractions of Ca remaining after loss of secondary calcite between 0.21 and 0.48 (average 0.39) and silicate fractions of Sr, Ca and Mg of ~34, 12 and 42% (Electronic Annex, Table E9).

7. RESULTS: MODELLING FLOOD PLAIN WEATHERING FLUXES

7.1. Chemical fluxes calculated by outputs of flood plain rivers and the difference between the major rivers entering the flood plain and the Ganga at Farakka

The simplest measure of chemical weathering on the flood plain is the difference between the chemical fluxes delivered to the flood plain (Tables 2 and 3) and those carried by the Ganga at Farakka.

The mean discharge from the flood plain, calculated from the difference between the inputs and the Ganga discharge at Farakka, is 7.3×10^{10} m^3/yr. However this is the difference between two larger fluxes, the input from the Himalayas and the southern rivers totalling ~2.8×10^{11} m^3/yr and the output at Farakka of 3.77×10^{11} m^3/yr and therefore the value is sensitive to uncertainties in both these values. Further evapo-transpiration enhanced by extraction for irrigation likely removes some of the water input from the Himalayas and southern rivers as they traverse the flood plain so that the total water input from the mountains, southern rivers and rain exceeds the discharge at Farakka. Average rainfall in the Ganga flood plain is ~1 m/yr (Bookhagen and Burbank, 2010) and allowing for loss by evapo-transpiration of between 50 and 75% (e.g. Rai et al., 2010) this would imply rain water inputs to the flood plain of ~1.75 to 1.0×10^{11} m^3/yr.

The mean output from the flood plain calculated as the difference between the chemical fluxes at Farakka and the chemical inputs from the Himalayas and the Southern rivers is given in Table 4. The uncertainties in Table 4 reflect the uncertainties in concentration and discharge. The latter are taken as 25% for the southern rivers (the discharge data are poorly documented) and as given in Table 2 for the mountain rivers. The uncertainty in the calculated $^{87}Sr/^{86}Sr$ ratio, which reflects uncertainties in both Sr fluxes and $^{87}Sr/^{86}Sr$ ratios of the rivers, is too large to be useful. The uncertainties in the fluxes of the elements are about 40% at 1σ except Si and Sr (~100%).

Given the mean output chemical fluxes and water flux from the flood plain calculated from the difference in discharges from the Himalayas and the southern rivers and that at Farakka, the implied concentrations of the flood plain inputs of Na, Ca and Mg are about 50% higher than the mean concentrations in the flood plain rivers (compare Tables 1 and 4). This may reflect two factors. The flood plain rivers were sampled during August at high flow when concentrations would be lower than average (discharge-weighted concentrations in the Ganga at Farakka are higher by 36% for Na, 10% for Ca, 25% for Mg and 13% for Sr than the August values). The second factor, as discussed above, is the loss of water in the flood plain by evaporation. However the uncertainties in this method of calculation are high.

7.2. Flood plain weathering fluxes calculated by deconvolution of chemical and isotopic inputs

An alternative and preferred method for calculation of chemical weathering inputs from the flood plain is deconvolution of the chemical and water inputs from the Himalayan mountain rivers, the southern tributaries and the flood plain based only on mass balance of the solute and Sr-isotopic compositions. This method has the advantage that it does not depend on the very uncertain discharge estimates for the Himalayan and southern rivers. Mass balance for the concentration of component, i, in the Ganga at Farakka, X^i_G, may be related to the sum of the mean concentrations of the component in the Himalayan rivers, southern rivers and flood plain runoff as

$$X^i_G = P_M \cdot X^i_M + P_S \cdot X^i_S + P_{Fl} \cdot X^i_{Fl} \quad (5)$$

where P_M, P_S and P_{Fl} are the discharges from the Himalayas, southern rivers and flood plain relative to that at Farakka and X^i_M, X^i_S, X^i_{Fl} are the concentrations (μmol/L except Sr nmol/L) of component, i, in the Himalayan, southern (based on adjusted monsoon compositions) and the flood plain rivers (all uncorrected for saline inputs). The mass-balance of Sr-isotopic compositions is calculated from $Sr{\cdot}\Delta^{87}Sr$ which is a measure of the relative forcing factors of the river inputs on the $^{87}Sr/^{86}Sr$ ratio in the Ganga. $Sr{\cdot}\Delta^{87}Sr$ is defined as

$$Sr \cdot \Delta^{87}Sr = Sr\left(^{87}Sr/^{86}Sr - {}^{87}Sr/^{86}Sr_F\right) \quad (6)$$

where $^{87}Sr/^{86}Sr_F$ is the mean Sr-isotopic composition of the Ganga at Farakka and mass balance for Sr-isotopic compositions can be written

$$Sr_G \cdot \Delta^{87}Sr_G = P_M \cdot Sr_M \cdot \Delta^{87}Sr_M + P_S \cdot \Delta Sr_S \cdot {}^{87}Sr_S + P_{Fl} \cdot Sr_{Fl} \cdot \Delta^{87}Sr_{Fl} \quad (7)$$

Note that the sum of the fractional discharges, P_M, P_S and P_{Fl}, may not be equal to unity because the waters that cross the flood plain may be diluted by additional rainfall or concentrated by evapo-transpiration in the flood plain as discussed above. Eqs. (5) and (7) are solved for P_M, P_S and P_{Fl} for three or more elements/isotopes by the linear least-squares routines from Kent et al. (1990) which propagate uncertainties on all the concentrations $X^i_G, X^i_M, X^i_S, X^i_{Fl}$.

The results calculated for various combinations of components are listed in Electronic annex Table E10. The best

Table 4
Estimates of floodplain outputs and discharge-weighted compositions.

Sample	Na	1σ	K	1σ	Ca	1σ	Mg	1σ	Si	1σ	Cl	1σ	SO_4	1σ	Sr[a]	1σ	$^{87}Sr/^{86}Sr$[a]		Discharge	
Floodplain estimates	10^9 mol/yr (flux), μmol/L (concentration)																	1σ	10^9 m^3/yr	1σ
Flux by simple difference[b]	62	23	15	4	98	40	45	16	12	9	25	8	11	6	98	73			73	55
Concentration by difference[b]	853	312	202	60	1338	542	620	214	165	128	345	108	151	85	1332	989	0.8145	38.53		
Flux from chemical budgets[c]	66	18	13	4	109	24	57	13	30	6	-	-	15	3	167	38	0.7304	0.0008	163	36
Flux from river sediments[f]	53	18	42	13	199	100	86	32							*188*	*57*	*0.737*	*0.013*		
Input/output fluxes																				
Himalayas[d]	19	4	9	2	101	19	38	7	21	4	4	1	26	5	151	29	0.7330	0.0012	190	42
Southern rivers[d]	35	9	4	1	44	12	16	4	14	4	11	3	4	1	109	30	0.7138	0.0016	65	19
Ganga at Farakka[e]	137	9	32	2	274	17	111	7	56	4	48	3	44	3	429	27	0.72662	0.00040	377	47

[a] Sr fluxes 10^9 mmol/yr, concentrations nmol/L. Floodplain.

[b] Output flux from floodplain calculated from difference between inputs from Himalayas and Southern rivers and output of Ganga at Farakka. 1σ uncertainties reflect uncertainties in concentrations and discharge.

[c] Output discharge and chemical fluxes from floodplain calculated by mass balance of Na, K, Ca, Mg, SO_4, Sr and $Sr{\cdot}\Delta^{87}Sr$ fluxes (Eq. (7)) (with saline inputs subtracted after calculation to make comparable to estimates from river sediments) relative to discharge and chemical fluxes of Ganga at Farakka. Uncertainties reflect uncertainty in input compositions and in flux.

[d] Chemical fluxes in Himalayan rivers and southern rivers calculated from the discharge calculated by deconvolution of chemistries as for 'c' and their mean compositions as given in Tables 1 and 2 (note these discharges are similar to but not identical to those tabulated in Tables 1 and 2 and used for the calculation by difference and that saline inputs have not been subtracted).

[e] Chemical fluxes in Ganga at Farakka calculated from discharge-weighted mean composition (Table 3) and the mean annual discharge of 377×10^9 m^3/yr from Hossain et al. (1987) with uncertainties reflecting variability in both chemistry and discharge over 3 year sample period.

[f] Floodplain chemical weathering fluxes calculated from the change in riverine sediment compositions by Lupker et al. (2012a). Sr flux and $^{87}Sr/^{86}Sr$ ratio calculated from river Ca and Na fluxes given by Lupker et al. (2012a). Sr flux calculated assuming all of Ca flux is from carbonate with a Sr/Ca ratio of 0.47 mmol/mol and Sr from silicate with a Sr/Na ratio of 1.8 mmol/mol from leaching bedload (Electronic appendix S2).

fit with the smallest propagated errors is given by the combination Na, K, Ca, Mg, SO_4, Sr and $Sr{\cdot}\Delta^{87}Sr$. The quality of the fits is described by the mean square of the weighted deviate (MSWD, see Albarède, 1995) which is a measure of the scatter in excess of the estimated errors. A fit in which scatter matches the estimated errors gives a fit with MSWD = 1. Inclusion of Si or Cl substantially degrades the quality of the fits with MSWD increasing from <2 to 8 or 12 and the uncertainties on the fits ~100%. Using only four components out of Na, Ca, Mg, Sr and $Sr.\Delta^{87}Sr$ gives results within error of regressions with the 6 or 7 components. The results consistently give total discharge ($\sum P_i$) ~ 11 ± 5% greater than the discharge at Farakka which likely reflects evapo-transpiration losses in the flood plain as discussed above. The calculated discharges from the Himalayas (192×10^9 m^3/yr) and southern rivers (66×10^9 m^3/yr), relative to the discharge at Farakka given by Hossain et al. (1987) are within the uncertainties of the values compiled in Tables 2 and 3. The calculated discharge from the flood plain (160×10^9 m^3/yr) is within the range expected from the rainfall and the rather uncertain magnitude of evapo-transpiration as discussed above.

Calculation of the relative discharges for each month throughout the year using the monthly averages at Farakka for the outputs from the flood plain is not possible because the compositions of the monthly Himalayan and southern river inputs are not known.

8. DISCUSSION: MAGNITUDE OF FLOOD PLAIN CHEMICAL WEATHERING FLUXES

We consider that the best estimate of the discharge and chemical fluxes from the flood plain is that calculated by deconvolution of the chemical and Sr-isotopic data because this does not rely on the very uncertain estimates of the river discharges and allows for water loss by evapo-transpiration on the flood plain. The calculated uncertainties should be regarded as minimum estimates because the averages of nearly all the Himalayan and southern tributaries and flood plain waters do not include adequate time-series sets to capture the full annual variability.

The flood plain weathering fluxes calculated here range from 41% for Sr to 63% for Na (corrected for saline inputs) of the calculated total elemental fluxes from the mountains, floodplain and the southern rivers (Fig. 16A). Even if the lower estimates from the differences in discharge are adopted (Table 4) the flood plain weathering fluxes range from 28% for Sr to 41% for Na. Given that nearly all the flood plain comprises sediment from the Himalayas (Lupker et al., 2012b), these values imply that ~59% Sr, 53% Ca, 60% Mg and 82% of the Na derived from Himalayan detritus is supplied by weathering in the flood plain, confirming its importance to the overall chemical weathering budget.

K, Si and Cl exhibit the largest deficit between the observed chemical flux at Farakka and that inferred from compositional deconvolution of the water compositions. The implication is that significant K and Cl (10 and 23% of the Ganga flux) is derived from the flood plain in excess of that carried by the analysed flood plain, Himalayan and southern river waters. The 23% deficit of Si in the Ganga waters suggests that Si is precipitated in the flood plain consistent with the interpretation of the Si-isotopic systematics (Fontorbe et al., 2013). There have been relatively few previous attempts to calculate the chemical weathering yields from the Ganga flood plain. Galy and France-Lanord (1999) estimated from the difference between the input and output fluxes, that the flood plain provided 14% of the Na, 41% of the K, 18% of the Ca in the downstream Ganga but that 14% of Mg was taken up by the flood plain. West et al. (2002) estimated that weathering of High Himalayan silicate material in the flood plain occurs at two and a half to six-times the rate in the mountains, again from differences in input and output river chemistries. Rai et al.'s (2010) estimates of weathering fluxes on the Ganga flood plain indicated that inputs exceeded outputs for Na, Mg, Sr, Si, Cl and SO_4 and were within error for Ca but these budgets were based mainly on May and October samples. Also, as noted here, the relatively small difference between the discharge in the downstream Ganga and the inputs to the flood plain as well as the potential for water loss by evapo-transpiration makes calculation of the flood plain flux by difference unreliable.

Lupker et al. (2012a) calculated flood plain chemical weathering inputs by the difference in riverine sediment loads at the margins of the flood plain and the Ganga in Bangladesh. Given the careful sampling of the riverine sediment, this method is attractive because it averages sediment compositions over much longer time scales than the water sampling. The difficulty is that the changes in sediment composition are small given the scatter in sediment compositions and the resulting flux estimates have large uncertainties for some elements (Table 4).

The flood plain chemical weathering fluxes of Na, K, Ca and Mg calculated from the water data here after allowance for inputs from saline sources (Na 66 ± 16, K 13 ± 4, Ca 109 ± 22, Mg 57 ± 13 × 10^9 mol/yr, 1σ errors) are within error of those calculated by the change in composition of sediments transported by the rivers across the flood plain (Na 53 ± 18, K 42 ± 13, Ca 199 ± 100, Mg 86 ± 32 × 10^9 mol/yr) by Lupker et al. (2012a) (Table 4). If it is assumed that the loss of ~50% of Ca to secondary calcite is not returned to solution then the chemical weathering flux of Ca in the flood plain should be increased to ~220 × 10^9 mol/yr. The Mg and Sr fluxes should be increased by about 5%. The comparison indicates that the current short-term estimates based on water chemistries are compatible with the longer-term estimates based on changes in sediment chemistry which sample chemical weathering over thousands or tens of thousands of years (e.g. Lupker et al., 2012b; Granet et al., 2010) and predate the development of intensive agriculture, but note the uncertainties. The silicate-derived flux of Ca is small (ca. 20 × 10^9 mol/yr allowing for loss to secondary calcite), and Mg (27 × 10^9 mol/yr) is modest.

The total chemical weathering fluxes and the fractions derived from salts (rain and evaporates or springs), carbonate minerals and silicate minerals for the inputs from the Himalayan mountains, the southern rivers and the floodplain, calculated as discussed above, are illustrated in

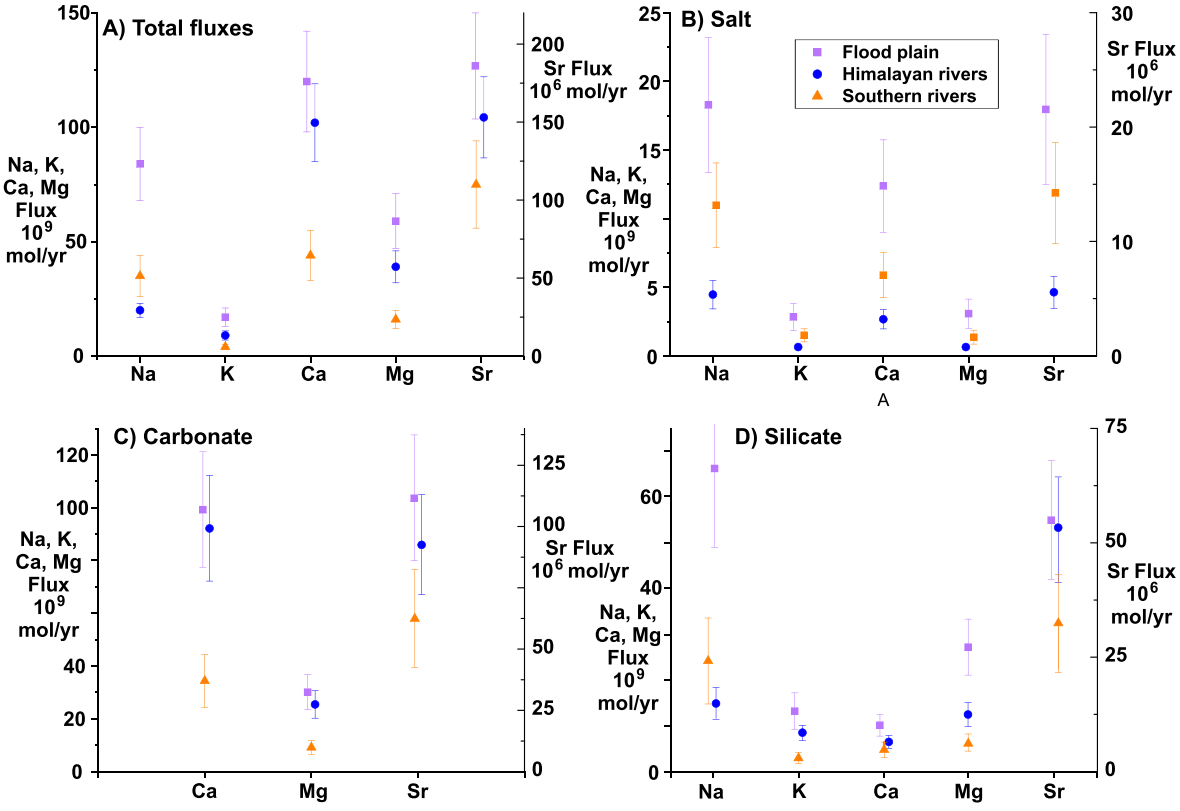

Fig. 16. Chemical fluxes from the flood plain, Himalayan rivers and southern rivers calculated from chemistry of inputs compared to chemistry of Ganga at Farakka (Eq. (5)) scaled to discharge of Ganga. (A) gives total flux from each source, (B) flux from rain and spring or evaporate source, (C) carbonate minerals and (D) silicate minerals.

Fig. 16. The significance of the chemical weathering in the floodplain is demonstrated by the estimates for the silicate inputs of Na, K, Ca and Mg all being equal or greater in the floodplain than inputs in the mountains (Fig. 16D). Inputs of Ca, Mg and Sr from weathering of carbonate minerals from the mountains and the floodplain are similar and between a factor of two to three greater than inputs from the southern rivers. The similarity between the estimates of the Na dissolved flux from the floodplain from the water chemistries and from the change in suspended load chemistries suggests that short-term variations in inputs from Na salts on the flood plain are insignificant within the error bounds.

The important conclusion is that chemical weathering in the floodplain more than doubles the impact of the rapid erosion and chemical weathering in the Himalayas. This estimate of weathering in flood plain is larger than that of Galy and France-Lanord (1999) and reflects in part significantly higher estimates of the flux-weighted mean compositions of Na, K, Ca and Mg in the downstream Ganga based on the three years time-series sampling. Chemical weathering in the flood plain must take place in the sediments stored on the flood plain and the comparison between the chemical fluxes calculated from the water chemistries and the suspended load compositions confirms the contention of Lupker et al. (2012a) that the suspended load in the the Ganga in Bangladesh is representative of the weathering on the flood plain. It is also consistent with the calculation by Lupker et al. (2012b) that the 90% of the sediment delivered to the flood plain, that is subsequently exported to the Bay of Bengal, is recycled with a ~1400 year time constant.

The preservation of significant plagioclase (~10 wt% in the suspended and bedloads of the Ganga in Bangladesh (Garzanti et al., 2010, 2011) indicates that weathering on the flood plain is incomplete. This is supported by the fractions of the major cations leached from the solid load. Taking (1) Lupker et al.'s. (2012b) estimate that the Ganga sediment flux in Bangladesh is 610 ± 210 Mt/yr from ^{10}Be analyses and that this is generated almost entirely in the Himalayan mountains, (2) that the average composition of the source rock is given by the mean of the suspended and bedload samples from the mountain rivers compiled by Lupker et al. (2012a) with a small adjustment to this composition for the chemical weathering flux from the mountains, and combined with (3) the chemical weathering fluxes calculated from the water chemistries, implies that the Himalayan-derived silicate sediment has lost only ~28% of Na, 6% of K, 18% of Ca and 15% of Mg by the time it reaches Bangladesh. The loss of 28% Na is consistent with the 25% decrease in Na/Si ratio of the suspended sediment between the Himalayan mountain front and Bangladesh noted by Lupker et al. (2012a). On a mass basis the total dissolved solids ($Na_2O + K_2O + CaO + MgO + SiO_2 + Cl + SO_4$) carried by the Ganga at Farakka comprises only ~5.7% of the solid load (2.7% added in the

floodplain, 2% in the Himalayan mountains and 1% from the southern rivers). Chemical weathering in the Ganga floodplain is 'weathering limited' (sense Stallard and Edmond, 1983), as in the mountains, and the consequence is that chemical weathering fluxes from both regions are predicted to be sensitive to changing climatic conditions (cf. West et al., 2005).

The Ganga river system illustrates the complexity of deciphering controls on chemical weathering fluxes. West et al. (2005) showed that both the High Himalayan and Lesser Himalayan catchments were 'weathering limited'. Discharge and erosion rate data from the Marsyandi Tibetan Sedimentary Series catchment in Nepal (Bickle et al., 2015; Gabet et al., 2008) exhibits a similar physical and silicate chemical weathering relationship (Fig. 17). The silicate cation denudation rate for the whole Ganga catchment, calculated for the area of the Himalayan mountains which dominate the supply of sediment, also lies in the 'weathering limited' field, albeit with a substantially increased silicate weathering flux (Fig. 17). The increased silicate weathering flux reflects the weathering in the flood plain and also additions from the southern tributaries. It is probable that chemical weathering in the catchments of the southern tributaries is transport limited but constraints on the rates of physical denudation there are not available. The output from the whole Ganga catchment therefore reflects sub-catchments which range from 'weathering limited' to 'transport limited' and processing of partially weathered material in the flood plain. Evaluating the response of silicate chemical weathering fluxes to changing climatic parameters in such a complex catchment is clearly complicated. For example increased temperatures and rainfall will increase the chemical flux from the mountainous catchments but supply of the more weathered material might limit chemical weathering on the flood plain. The response of the floodplain weathering to changes in temperature and especially rainfall is likely to differ from that of the mountainous catchments as groundwater flow paths and flow rates are likely to be very different.

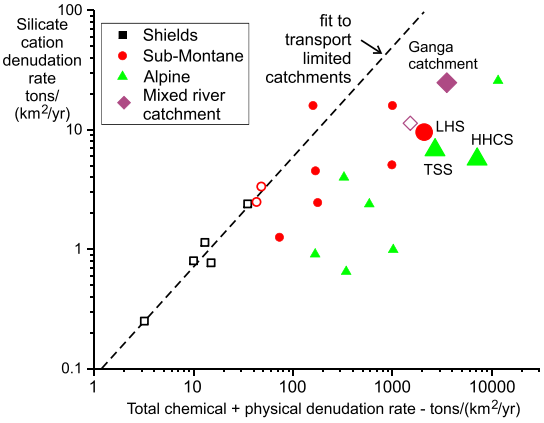

Fig. 17. Silicate cation denudation rates versus total denudation rate for catchments listed by West et al. (2005) with addition of data from the Marsyandi catchment in the Tibetan Sedimentary series using the estimates of silicate chemical fluxes by Bickle et al. (2015) and physical denudation fluxes by Gabet et al. (2008). The estimate for the whole Ganga catchment is based on the silicate chemical fluxes given here and the physical denudation rate of the whole Ganga catchment by Lupker et al. (2012b). The Ganga weathering rates (solid symbol) are normalised to the area of the Himalayas as that area dominates the supply of rock. The open symbol illustrates the Ganga silicate chemical and total denudation rates normalised to the whole catchment above Farakka.

9. CONCLUSIONS

Tributaries to the Ganga which are restricted to the flood plain have chemistries and oxygen and hydrogen isotopic compositions which are distinct from the major rivers rising in the Himalayas and Tibet. The $\delta^{18}O$ - δD arrays (i.e. $\delta D_{excesses}$) of the flood plain tributaries reflect evaporative loss from the flood plain which is reflected in the higher $\delta D_{excesses}$ of the mountain rivers.

The flood plain tributaries may be divided into two distinct groups on the basis of their Sr-isotopic compositions and Sr/Ca to Na/Ca arrays. Over most of the flood plain tributaries have $^{87}Sr/^{86}Sr$ ratios < 0.75 and Na/Ca molar ratios < 1.0 except for a small subset of samples close to the Gomti river with elevated Na concentrations thought to be derived by re-dissolution of Na-salts. However in the east of the flood plain, in a restricted area around the Kosi, waters have $^{87}Sr/^{86}Sr$ ratios greater than 0.75 and higher Na/Ca ratios which correlate with Sr/Ca ratios. The bed load compositions of these tributaries are consistent with the high $^{87}Sr/^{86}Sr$ ratios being derived from both high $^{87}Sr/^{86}Sr$ dolomites and even higher $^{87}Sr/^{86}Sr$ ratio silicate minerals from Lesser Himalayan Series.

Modelling of the Sr-isotopic compositions of the flood plain tributaries allows calculation of the inputs of carbonate and silicate Sr. It also provides estimates of the fractions of Ca, Sr and Mg lost to precipitation of secondary calcite within the flood plain. The fractions of Ca remaining after precipitation range from ~24% to 91% in individual tributaries with a mean of between 36 and 57% depending on the estimate of carbonate Sr/Ca and silicate $^{87}Sr/^{86}Sr$ ratios. The modelling takes the Sr-isotopic compositions and Sr/Ca ratio of the carbonate input from leaches of mainstem Ganga bedloads and the silicate $^{87}Sr/^{86}Sr$, Na/Ca and Na/Mg ratios from analyses of residues of bedloads after leaching. After correction for rain and saline inputs, ~31% of the Sr, 8% of the Ca and 45% of the Mg are estimated to be derived from silicate. It should be noted that the calculations imply substantial ranges for the Mg/Ca ratios of carbonate inputs and Sr/Ca ratios of silicate inputs across the individual tributaries. The impact of assuming single values of Sr/Ca ratios for the carbonate inputs and $^{87}Sr/^{86}Sr$, Na/Ca and Mg/Ca ratios for silicate inputs is uncertain.

Calculation of the chemical weathering fluxes from the flood plain by difference between the chemical fluxes in the downstream Ganga and the inputs from the Himalayan mountains and southern tributaries gives combined uncertainties in chemical compositions and water fluxes are of the same order as the difference. Deconvolution of the fluxes using the average chemistries of the mountain rivers, the southern rivers and the downstream Ganga sampled at

Farakka, with flood plain outputs characterised by the flood plain tributaries, is preferred. This defines Na, K, Ca, Mg, SO_4 and Sr fluxes with 1 sigma uncertainties of about 30%. Calculated input water fluxes are about 10% greater than the discharge in the downstream Ganga attributed to evaporation and transpiration as water crosses the flood plain.

Two factors dominate the uncertainties of fluxes calculated from analyses of river water compositions. (1) Most of the major rivers from the Himalayas and all of the southern rivers have only been sampled on relatively few occasions whereas repeated bi-weekly sampling over several years is required to properly constrain the average chemistry in rivers which exhibit large seasonal changes in water chemistries. (2) Calculation of annual discharges requires knowledge of discharge throughout the season, information which is only sparingly available for major Indian rivers.

Weathering in the flood plain supplies between 41 and 63% of the major cation and Sr fluxes carried by the Ganga compared to between 14% (Na) and ~36% (Sr) supplied by the major Himalayan rivers (Table 4). The flood plain supplies 58%, the Himalayan rivers 24% and the southern rivers 18% of the silicate weathering-associated alkalinity flux carried by the Ganga at Farakka. Weathering in the Ganga flood plain makes a dominant contribution to weathering of material eroded from the Himalayan mountains.

ACKNOWLEDGEMENTS

The research was supported by the UK Natural Environment Research Council grants (NE/E003192/1 and NE/N007441/1). Dr Jyotisankar Ray (University of Calcutta, India) helped organise the sampling of the Ganga at Farakka. The late Dr Fatima Khan gave extensive assistance with the chemical and isotopic analyses. D. Hodell provided the δD and $\delta^{18}O$ analyses. We acknowledge constructive reviews by the associate editor, T.K. Dalai and an anonymous reviewer.

APPENDIX A. SUPPLEMENTARY MATERIAL

Supplementary data associated with this article can be found, in the online version, at https://doi.org/10.1016/j.gca.2018.01.003.

REFERENCES

Albarède F. (1995) *Introduction to Geochemical Modeling*. Cambridge University Press, Cambridge.

Andermann C., Longuevergne L., Bonnet S., Crave A., Davy P. and Gloaguen R. (2012) Impact of transient groundwater storage on the discharge of Himalayan rivers. *Nat. Geosci.* **5**, 127–132.

Battacharya S. K., Gupta S. K. and Krishnamurthy R. V. (1985) Oxygen and hydrogen isotopic ratios in groundwaters and river waters from India. *Proc. Indian Acad. Sci. (Earth Planet. Sci.)* **94**, 283–295.

Becker J. A., Bickle M. J., Galy A. and Holland T. J. B. (2008) Himalayan metamorphic CO_2 fluxes: Quantitative constraints from hydrothermal springs. *Earth Planet. Sci. Lett.* **265**, 616–629.

Berner R. A., Lasaga A. C. and Garrels R. M. (1983) The carbonate-silicate geochemical cycle and its effect on atmospheric carbon dioxide over the past 100 million years. *Am. J. Sci.* **283**, 641–683.

Bhargava G. P., Paul D. K., Kapoor B. S. and Goswami S. C. (1981) Characteristics and genesis of some sodic soils in the Indo-Gangetic alluvial plain of Haryana and Uttar Pradesh. *J. Indian Soc. Soil Sci.* **29**, 60–71.

Bickle M. J. (1996) Metamorphic decarbonation, silicate weathering and the long-term carbon cycle. *Terra Nova* **8**, 270–276.

Bickle M. J., Harris N. B. W., Bunbury J., Chapman H. J., Fairchild I. J. and Ahmad T. (2001) Controls on the $^{87}Sr/^{86}Sr$ of carbonates in the Garwal Himalaya, headwaters of the Ganges. *J. Geol.* **109**, 737–753.

Bickle M. J., Bunbury J., Chapman H. J., Harris N. B., Fairchild I. J. and Ahmad T. (2003) Fluxes of Sr into the headwaters of the Ganges. *Geochim. Cosmochim. Acta* **67**, 2567–2584.

Bickle M. J., Chapman H. J., Bunbury J., Harris N. B. W., Fairchild I. J., Ahmad T. and Pomiès C. (2005) The relative contributions of silicate and carbonate rocks to riverine Sr fluxes in the headwaters of the Ganges. *Geochem. Cosmochim. Acta* **69**, 2221–2240.

Bickle M. J., Tipper E. D., Galy A., Chapman H. J. and Harris N. W. B. (2015) On discrimination between carbonate and silicate inputs to Himalayan rivers. *Am. J. Sci.* **315**, 120–166.

Bookhagen B. and Burbank D. W. (2010) Toward a complete Himalayan hydrological budget: Spatiotemporal distribution of snowmelt and rainfall and their impact on river discharge. *J. Geophys. Res.* **115**, F03019 03025.

Bouchez J., Gaillardet J., Lupker M., Louvat P., France-Lanord C., Laurence Maurice L., Armijos E. and Moquet J.-S. (2012) Flood plains of large rivers: Weathering reactors or simple silos? *Chem. Geol.* **332–333**, 166–184.

Brady P. V. and Gislason S. R. (1997) Seafloor weathering controls on atmospheric CO_2 and global climate. *Geochim. Cosmochim. Acta* **61**, 965–973.

Caldeira, K., Arthur, M.A., Berner, R.A., & Lasaga, A.C. (1993). Cooling in the Cenozoic: Discussion of 'Tectonic forcing of late Cenozoic climate' by Raymo, M.E. and Ruddiman, W.F. Nature 361, 123–124.

Calmels D., Galy A., Hovius N., Bickle M., West A. J., Chen M. C. and Chapman H. (2011) Contribution of deep groundwater to the weathering budget in a rapidly eroding mountain belt, Taiwan. *Earth Planet. Sci. Lett.* **303**, 48–58.

Carson M. A. and Kirby M. J. (1972) *Hillslope, Form and Process*. Cambridge University Press, Cambridge.

Chamberlin T. C. (1899) The influence of great epochs of limestone formation upon the constitution of the atmosphere. *J. Geol.* **6**, 609–621.

Chapman H. J., Bickle M., Thaw S. H. and Thiam H. N. (2015) Chemical fluxes from time series sampling of the Irrawaddy and Salween Rivers, Myanmar. *Chem. Geol.* **401**, 15–27.

Coogan L. A. and Dosso S. E. (2015) Alteration of ocean crust provides a strong temperature dependent feedback on the geological carbon cycle and is a primary driver of the Sr-isotopic composition of seawater. *Earth Planet. Sci. Lett.* **415**, 38–46.

Cox K. G. and Hawkesworth C. J. (1985) Geochemical stratigraphy of the Deccan Traps at Mahabaleshwar, Western Ghats, India, with implications for open system magmatic processes. *J. Petrol.* **26**, 355–377.

Craig H. (1961) Isotopic variations in meteoric waters. *Science* **133**, 1702–1703.

Craig H. and Gordon L. I. (1965) Deuterium and oxygen 18 variations m the ocean and the marine atmosphere. In *Stable isotopes in oceanographic studies and paleotemperatures* (ed. E. Tongiorgi). Consiglio nazionale delle Ricerche Laboratorio di Geologia Nucleare, Spoleto, pp. 9–130.

Dalai T. K., Krishnaswami S. and Sarin M. M. (2002) Major ion chemistry in the headwaters of the Yamuna river system: Chemical weathering, its temperature dependence and CO_2 consumption in the Himalaya. *Geochim. Cosmochem. Acta* **66**, 3397–3416.

Dalai T. K., Krishnaswami S. and Kumar A. (2003) Sr and $^{87}Sr/^{86}Sr$ in the Yamuna River System in the Himalaya: Sources, fluxes, and controls on Sr isotope composition. *Geochem. Cosmochim. Acta* **67**, 2931–2948.

Dansgard W. (1964) Stable isotopes in precipitation. *Tellus* **16**, 436–468.

Dessert C., Dupre B., Francois L. M., Schott J., Gaillardet J., Chakrapani G. and Bajpai S. (2001) Erosion of Deccan Traps determined by river geochemistry: impact on the global climate and the $^{87}Sr/^{86}Sr$ ratio of seawater. *Earth Planet. Sci. Lett.* **188**, 459–474.

Dawson T. E., Mambelli S., Plamboeck A. H., Templer P. H. and Tu K. P. (2002) Stable isotopes in plant ecology. *Annu. Rev. Ecol. Syst.* **33**, 507–559.

Edmond J. M. (1992) Himalayan tectonics, weathering processes, and the strontium isotope record in marine limestones. *Science* **258**, 1594–1597.

English N. B., Quade J., DeCelles P. G. and Garzione C. (2000) Geologic control of Sr and major element chemistry in Himalayan rivers, Nepal. *Geochim. Cosmochim. Acta* **64**, 2549–2566.

Fekete, B.M., Vorosmarty, C.J., Grabs, W., 2000. Global, composite runoff fields based on observed river discharge and simulated water balances, Documentation for UNH-GRDC Composite Runoff Fields, v. 1.0. Global Runoff Data Centre, Koblenz, Germany.

Fontorbe G., De La Rocha C. L., Chapman H. J. and Bickle M. J. (2013) The silicon isotopic composition of the Ganges and its tributaries. *Earth Planet. Sci. Lett.* **381**, 21–30.

France-Lanord F., Evans M., Hurtrez J.-E. and Riotte J. (2003) Annual dissolved fluxes from Central Nepal rivers: budget of chemical erosion in the Himalayas. *Compte Rendus Geosci.* **335**, 1131–1140.

Francois L. M. and Walker J. C. G. (1992) Modelling the phanerozoic carbon cycle and climate: constraints from the $^{87}Sr/^{86}Sr$ isotopic ratio of seawater. *Am. J. Sci.* **292**, 81–135.

Gabet E. J., Burbank D. W., Pratt-Sitaula B., Putkonen J. and Bookhagen B. (2008) Modern erosion rates in the High Himalayas of Nepal. *Earth Planet. Sci. Lett.* **267**, 482–494.

Gaillardet J., Dupre B., Louvat P. and Allegre C. J. (1999) Global silicate weathering and CO_2 consumption rates deduced from the chemistry of large rivers. *Chem. Geol.* **159**, 3–30.

Gajurel A. P., France-Lanord C., Huyghe P., Guilmette C. and Gurung D. (2006) C and O isotope compositions of modern fresh-water mollusc shells and river waters from the Himalaya and Ganga plain. *Chem. Geol.* **233**, 156–183.

Galy A. and France-Lanord C. (1999) Weathering processes in the Ganges-Brahmaputra basin and the river alkalinity budget. *Chem. Geol.* **159**, 31–60.

Galy A., France-Lanord C. and Derry L. A. (1999) The strontium isotopic budget of Himalayan Rivers in Nepal and Bangladesh. *Geochim. Cosmochim. Acta* **63**, 1905–1925.

Galy V., France-Lanord C., Beyssac O., Faure P., Kudrass H. and Palhol F. (2007) Efficient organic carbon burial in the Bengal fan sustained by the Himalayan erosional system. *Nature* **450**, 407–410.

Garçon M., Chauvel C., France-Lanord C., Limonta M. and Garzanti E. (2013) Removing the "heavy mineral effect" to obtain a new Pb isotopic value for the upper crust. *Geochem. Geophys. Geosyst.* **14**, 9. https://doi.org/10.1002/ggge.20219.

Garçon M., Chauvel C., France-Lanord C., Limonta M. and Garzanti E. (2014) Which minerals control the Nd–Hf–Sr–Pb isotopic compositions of river sediments? *Chem. Geol.* **364**, 42–45.

Garzanti E., Andó S., France-Lanord C., Vezzoli G., Censi P., Galy V. and Najman Y. (2010) Mineralogical and chemical variability of fluvial sediments 1. Bedload sand (Ganga–Brahmaputra, Bangladesh). *Earth Planet. Sci. Lett.* **299**, 368–381.

Garzanti E., Andó S., France-Lanord C., Censi P., Vignola P., Galy V. and Lupker M. (2011) Mineralogical and chemical variability of fluvial sediments 2. Suspended-load silt (Ganga–Brahmaputra, Bangladesh). *Earth Planet. Sci. Lett.* **302**, 107–120.

Granet M., Chabaux F., Stille P., Dosseto A., France-Lanord C. and Blaes E. (2010) U-series disequilibria in suspended river sediments and implication for sediment transfer time in alluvial plains: The case of the Himalayan rivers. *Geochim. Cosmochim. Acta* **74**, 2851–2865.

Gupta L. P. and Subramanian V. (1994) Environmental geochemistry of the River Gomti: A Tributary of the Ganges River. *Environ. Geol.* **24**, 235–243.

Hodell D., Turchyn A., Wiseman C., Escobar J., Curtis J., Brenner M., Gilli A., Mueller A., Anselmetti F., Ariztegui D. and Brown E. (2012) Late Glacial temperature and precipitation changes in the lowland Neotropics by tandem measurement of $\delta^{18}O$ in biogenic carbonate and gypsum hydration water. *Geochim. Cosmochim. Acta* **77**, 352–368.

Hossain M., Aminul Islam A. T. M. and Kumar Saha S. (1987) *Floods in Bangladesh: Recurrent Disaster and People's Survival*. University Research Centre, Dhaka, Bangladesh, pp. 64–66.

Huh Y. (2010) Estimation of atmospheric CO_2 uptake by silicate weathering in the Himalayas and the Tibetan Plateau: a review of existing fluvial geochemical data. In *Geological Society* (eds. P. D. Clift, R. Tada and H. Zheng). London, Special Publications, London, pp. 129–151.

Jacobson A. D. and Blum J. D. (2000) Ca/Sr and $^{87}Sr/^{86}Sr$ geochemistry of disseminated calcite in Himalayan silicate rocks from Nanga Parbat: Influence on river water chemistry. *Geology* **28**, 463–466.

Jacobson A. D., Blum J. D. and Walter L. M. (2002) Reconciling the elemental and Sr isotope composition of Himalayan weathering fluxes: Insights from the carbonate chemistry of stream waters. *Geochim. Cosmochim. Acta* **66**, 3417–3429.

Jha P. K., Subramanian V. and Sitasawad R. (1988) Chemical and sediment mass transfer in the Yamuna River - a tributary of the Ganges system. *J. Hydrol.* **104**, 237–246.

Kent J., Watson G. and Onstott T. (1990) Fitting straight lines and planes with an application to radiometric dating. *Earth Planet. Sci. Lett.* **97**, 1–17.

Kerrick D. M. and Caldeira K. (1993) Paleoatmospheric consequences of CO_2 released during early Cenozoic regional metamorphism in the Tethyan orogen. *Chem. Geol.* **108**, 201–230.

Krishnamurthy, R., Bhattacharya, S. (1991). Stable oxygen and hydrogen isotope ratios in shallow ground waters from India and a study of the role of evapo-transpiration in the Indian monsoon. In: Taylor, H.P., O'Neil, J.R., Kaplan, R., (Eds.), Stable Isotope Geochemistry: A Tribute to Samuel Epstein, Geochem. Society, Special Publication, pp. 187–203.

Krishnaswami S., Trivedi J. R., Sarin M. M., Ramesh R. and Sharma K. K. (1992) Strontium isotopes and rubidium in the Ganga-Brahmaputra river system: weathering in the Himalaya, fluxes to the Bay of Bengal and contributions to the evolution of oceanic $^{87}Sr/^{86}Sr$. *Earth Planet. Sci. Lett.* **109**, 243–253.

Kumar B., Rai S. K., Saravana Kumar U., Verma S. K., Garg P., Vijaya Kumar S. V., Jaiswal R., Purendra B. K., Kumar S. R. and Pande N. G. (2010) Isotopic characteristics of Indian precipitation. *Water Resour. Res.* **46**, W12548.

Li D. D., Jacobson A. D. and McInerney D. J. (2014) A reactive-transport model for examining tectonic and climatic controls on chemical weathering and atmospheric CO_2 consumption in granitic regolith. *Chem. Geol.* **365**, 30–42.

Lupker M., Christian France-Lanord C., Valier Galy V., Lavé J., Gaillardet J., Gajurel A. P., Guilmette C., Rahman M., Singh S. K. and Sinha R. (2012a) Predominant flood plain over mountain weathering of Himalayan sediments (Ganga basin). *Geochim. Cosmochim. Acta* **84**, 410–432.

Lupker M., Blard P.-H., Lavé J., France-Lanord C., Leanni L., Puchol N., Charreau J. and Bourles D. (2012b) ^{10}Be-derived Himalayan denudation rates and sediment budgets in the Ganga basin. *Earth Planet. Sci. Lett.* **333–334**, 146–156.

Maher K. (2011) The role of fluid residence time and topographic scales in determining chemical fluxes from landscapes. *Earth Planet. Sci. Lett.* **312**, 48–58.

McKenzie N. R., Hughes N. C., Myrow P. M., Xiao S. and Sharma M. (2011) Correlation of Precambrian-Cambrian sedimentary successions across northern India and the utility of isotopic signatures of Himalayan lithotectonic zones. *Earth Planet. Sci. Lett.* **312**, 471–483.

Mondal M. E. A., Goswami J. N., Deomurari M. P. and Sharma K. K. (2002) Ion microprobe ^{207}Pb/^{206}Pb ages of zircons from the Bundelkhand massif, northern India: implications for crustal evolution of the Bundelkhand-Aravalli protocontinent. *Precambr. Res.* **117**, 85–100.

Pal D. K., Srivastava P., Durge S. L. and Bhattacharyya T. (2003) Role of microtopography in the formation of sodic soils in the semi-arid part of the Indo-Gangetic Plains, India. *Catena* **51**, 3–31.

Pal S. K. (1986) *Geomorphology of River Terraces Along the Alaknanda Valley, Garhwal Himalaya*. B.R. Publishing Corporation, Delhi-110052.

Palmer M. R. and Edmond J. M. (1992) Controls over the strontium isotope composition of river water. *Geochim. Cosmochim. Acta* **56**, 2099–2111.

Peng Z. X., Mahoney J. J., Hooper P. R., Macdougall J. D. and Krishnamurthy P. (1998) Basalts of the northeastern Deccan Traps, India: Isotopic and elemental geochemistry and relation to southwestern Deccan stratigraphy. *J. Geophys. Res.* **103**, 29,843-829,865.

Pogge von Strandmann P. A. E. and Henderson G. M. (2015) The Li isotope response to mountain uplift. *Geology* **43**, 67–70.

Quade J., English N. and DeCelles (2003) Silicate versus carbonate weathering in the Himalaya: a comparison of the Arun and Seti River watersheds. *Chem. Geol.* **202**, 275–296.

Rai S. K., Singh S. K. and Krishnaswami S. (2010) Chemical weathering in the plain and peninsular sub-basins of the Ganga: Impact on major ion chemistry and elemental fluxes. *Geochim. Cosmochem. Acta* **74**, 2340–2355.

Rao K. L. (1975) *India's Water Wealth*. Orient Longman Ltd., New Delhi.

Ray J. S., Veizer J. and Davis W. J. (2003) C, O, Sr and Pb isotope systematics of carbonate sequences of the Vindhyan Supergroup, India: age, diagenesis, correlations and implications for global events. *Precambrian Res.* **121**, 103–140.

Raymo M. E. and Ruddiman W. F. (1992) Tectonic forcing of late Cenozoic climate. *Nature* **359**, 117–122.

Raymo M. E., Ruddiman W. F. and Froelich P. N. (1988) Influence of late Cenozoic mountain building on ocean geochemical cycles. *Geology* **16**, 649–653.

Rengarajan R., Singh S. K., Sarin M. M. and Krishnaswami S. (2009) Strontium isotopes and major ion chemistry in the Chambal River system, India: Implications to silicate erosion rates of the Ganga. *Chem. Geol.* **260**, 87–101.

Richter F. M., Rowley D. B. and DePaolo D. J. (1992) Sr isotope evolution of seawater: the role of tectonics. *Earth Planet. Sci. Lett.* **109**, 11–23.

Sarin M. M., Krishnaswami S., Dilli K., Somayajulu B. L. K. and Moore W. S. (1989) Major ion chemistry of the Ganga-Brahmaputra river system: weathering processes and fluxes to the Bay of Bengal. *Geochim. Cosmochim. Acta* **53**, 997–1009.

Singh S. K., Trivedi J. R., Pande K., Ramesh R. and Krishnaswami S. (1998) Chemical and strontium, oxygen, and carbon isotopic compositions of carbonates from the Lesser Himalaya: Implications to the strontium isotope composition of the source waters of the Ganga, Ghaghara, and the Indus rivers. *Geochim. Cosmochim. Acta* **62**, 743–755.

Singh K. P., Malika A., Mohana D. and Sinha S. (2004) Multivariate statistical techniques for the evaluation of spatial and temporal variations in water quality of Gomti River (India)—a case study. *Water Res.* **38**, 3980–3992.

Singh K. P., Malik A. and Sinha S. (2005a) Water quality assessment and apportionment of pollution sources of Gomti river (India) using multivariate statistical techniques - a case study. *Anal. Chim. Acta* **538**, 335–374.

Singh M., Sharma M. and Tobschall H. J. (2005b) Weathering of the Ganga alluvial plain, northern India: implications from fluvial geochemistry of the Gomati River. *Appl. Geochem.* **20**, 1–21.

Singh S., Rai S. K. and Krishnaswami S. (2008) Sr and Nd isotopes in river sediments from the Ganga Basin: Sediment provenance and spatial variability in physical erosion. *J. Geophys. Res.* **113**, pp. F03006, 03018.

Singh S., Singh M., Choudhary A. K., Saxena A., Singh I. B. and Jain A. K. (2009) Sr isotopic signature of the Ganga Alluvial Plain and its implication to Sr flux of the Ganga River System. *Indian J. Earth Sci. (Geol Rundsch)*, 0.1007/s00531-00009-00479-00534.

Sleep N. H. and Zahnle K. (2001) Carbon dioxide cycling and implications for climate on ancient Earth. *J. Geophys. Res.* **106**, 1373–1399.

Stallard R. F. and Edmond J. M. (1983) Geochemistry of the Amazon. 2. The influence of geology and weathering environment on the dissolved-load. *J. Geophys. Res.* **88**, 9671–9688.

Subramanian V., Sitasawad R., Abbas N. and Jha P. K. (1987) Environmental geology of the Ganga river basin. *J. Geol. Soc. India* **30**, 335–355.

Tipper E. T., Bickle M. J., Galy A., West A. J., Pomiès C. and Chapman H. J. (2006) The short term climatic sensitivity of carbonate and silicate weathering fluxes: Insight from seasonal variations in river chemistry. *Geochim. Cosmochim. Acta* **70**, 2737–2754.

Torres M. A., West A. J. and Li G. (2014) Sulphide oxidation and carbonate dissolution as a source of CO_2 over geological timescales. *Nature* **507**, 346–349.

Turchyn A. V., Tipper E., Galy A., Lo J. and Bickle M. J. (2013) Isotope evidence for secondary sulfide precipitation along the Marsyandi River, Nepal, Himalayas. *Earth Planet. Sci. Lett.* **374**, 36–46.

Walker J. C. G., Hays P. B. and Kasting J. F. (1981) A negative feedback mechanism for the long-term stabilisation of Earth's surface temperature. *J. Geophys. Res.* **86**, 9776–9782.

West A. J., Bickle M. J., Collins R. and Brasington J. (2002) A small catchment perspective on Himalayan weathering fluxes. *Geology* **30**, 355–358.

West A. J., Galy A. and Bickle M. (2005) Tectonic and climatic controls on silicate weathering. *Earth Planet. Sci. Lett.* **235**, 211–228.

White A. F. and Blum A. E. (1995) Effects of climate on chemical weathering in watersheds. *Geochim. Cosmochim. Acta* **59**, 1729–1747.

York D. (1969) Least squares fitting of a straight line with correlated errors. *Earth Planet. Sci. Lett.* **5**, 320–324.

Associate Editor: Andrew D. Jacobson